



Water masses seasonality and meteorological patterns drive the biogeochemical processes of a subtropical and urbanized watershed-bay-shelf continuum

Alex Cabral^{a,b,*}, Carla H.C. Bonetti^{a,c}, Luis H.P. Garbossa^d, Jurandir Pereira-Filho^e, Kelly Besen^f, Alessandra L. Fonseca^{a,c}

^a Programa de Pós-Graduação em Oceanografia, Universidade Federal de Santa Catarina, Florianópolis, Brazil

^b Department of Marine Sciences, University of Gothenburg, Gothenburg, Sweden

^c Coordenadoria Especial de Oceanografia, Universidade Federal de Santa Catarina, Florianópolis, Brazil

^d Empresa de Pesquisa Agropecuária e Extensão Rural de Santa Catarina, Florianópolis, Brazil

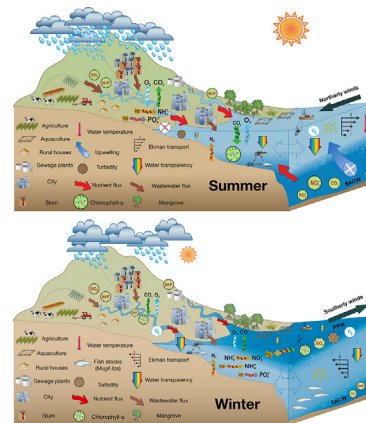
^e Escola do Mar, Ciência e Tecnologia, Universidade do Vale do Itajaí, Itajaí, Brazil

^f Departamento de Aquicultura, Universidade Federal de Santa Catarina, Florianópolis, Brazil

HIGHLIGHTS

- A subtropical bay is under eutrophication pressure due to sewage discharge.
- Meteo-oceanographic patterns shifted residence time and the ecosystem metabolism.
- Autotrophic conditions predominate in the summer and heterotrophic in the winter.
- El Niño and La Niña events modulate physical and biogeochemical processes.
- Assessment models indicated that the eutrophic conditions will persist.

GRAPHICAL ABSTRACT



ARTICLE INFO

Article history:

Received 12 December 2019

Received in revised form 3 August 2020

Accepted 5 August 2020

Available online 11 August 2020

Editor: Sergi Sabater

Keywords:

Nutrients
Chlorophyll-a
ENSO
TRIX

ABSTRACT

Understanding the different scales of temporal variability is crucial to improve the knowledge of the biogeochemical processes in the land-ocean interface. In this study, we evaluated the role of continental runoff and intrusion of oceanic water masses in the trophic state of the Bay of Santa Catarina Island (BSCI) over the last three decades (1993–2019) by using multiple biogeochemical and eutrophication assessment tools. The sub-watersheds of BSCI showed high concentrations of nutrients, fecal coliform and chlorophyll-a, directly correlated to the number of inhabitants. Worst-case scenarios were found in summer and fall seasons due to sewage inputs caused by mass tourism and the inefficiency or even absence of treatment systems, boosted by strong rainfall. The intrusion of the South Atlantic Central Water and the Plata Plume Water into the BSCI favored autotrophy in the summer and heterotrophy in the winter, coupled with low and high residence time, respectively. El Niño events enhanced rainfall and continental runoff, exporting elevated nutrients and phytoplankton biomass loads from the eutrophic rivers to the continental shelf. The pattern reverses during La Niña, when chlorophyll and nutrient peaks were detected inside the bay. Eutrophication evaluation indicated that the trophic state oscillated from moderate to high and

* Corresponding author at: Department of Marine Sciences, University of Gothenburg, Box 461, 40530 Gothenburg, Sweden.
E-mail address: alex.cabral@gu.se (A. Cabral).

that these conditions tend to remain the same in future scenarios due to the moderate residence time of the water, anthropogenic pressures, periodic algal blooms and the intrusion of nutrient-rich oceanic water masses. Management actions, such as the improvement of the wastewater treatment system and wetlands restoration, are needed in order to mitigate eutrophication and the loss of ecosystem services and functions.

© 2020 Elsevier B.V. All rights reserved.

1. Introduction

Estuaries are important transitional ecosystems and biogeochemical hotspots, where primary productivity and organic matter remineralization are enhanced by continental and oceanic fluxes (Bricker et al., 2008; Cloern et al., 2017). Disruptions in the natural processes are found when these systems are surrounded by urban or agricultural areas, activities that input high amounts of nutrients and other pollutants, mainly when wastewater treatment is not enforced or is poorly regulated (Cloern et al., 2016; Nixon, 2009). The allochthonous or autochthonous production of organic matter induced by anthropogenic nutrients is the main cause of eutrophication worldwide, especially in systems with low water exchange, such as lagoons and bays (Le Moal et al., 2019; Rabalais et al., 2010). There are many eutrophication symptoms in aquatic systems, such as algal blooms and deoxygenation, often leading to water quality degradation and loss of biodiversity and ecosystem services (Breitburg et al., 2018; Bricker et al., 2008).

The biogeochemical processes of coastal areas depends on multiple environmental and anthropic conditions, such as hydrological variability and watershed land-uses (Cloern et al., 2017; Dan et al., 2019; Li et al., 2012). Meteo-oceanographic events play an important role in this variability, such as the pulse of continental discharge induced by precipitation, increasing the trophic status of coastal systems (Brugnoli et al., 2019; Netto et al., 2018). Sometimes these events are coupled with large-scale phenomena (e.g. El Niño and La Niña), producing effects over weeks to months (Abreu et al., 2010; Cloern et al., 2016). In the subtropical region of Brazil, Ekman transport associated with persistent northerly winds drive surface waters away from the coast, triggering coastal upwelling events of the South Atlantic Central Water (SACW) in the euphotic zone (Bordin et al., 2019; Brandini et al., 2018). Southerly winds, on the other hand, force downwelling of surface ocean waters and storm surges over the coast, mainly in the winter (Möller et al., 2008). Southerly winds are also the main mechanism driving the meridional (from 34°S to ~24°S) displacement of the Plata Plume Water (PPW) through subtropical Brazil, producing strong physical and biogeochemical cross-shore gradients (Fontes et al., 2018; Pimenta and Kirwan, 2014).

Evaluate the biogeochemistry dynamics of coastal systems can be challenging due to the complex mechanisms described above. Long-term studies are essential to better understand the different scales of temporal and seasonal variability; however, there are few in South America (Abreu et al., 2010; Barrera-Alba et al., 2019; Cloern and Jassby, 2010; Ovalle et al., 2013). The Bay of Santa Catarina Island (BSCI, Fig. 1) has been showing eutrophication symptoms in the watersheds and shallow regions, such as algal blooms and hypoxia (Alves et al., 2010; Pagliosa et al., 2006; Silva et al., 2016). In addition, the sewerage systems are not effective since nutrient removal is low, also 56% of households use individual cesspools and just 27% of all domestic wastewater is processed by secondary treatment plant (ANA, 2017). Associated with this condition, we must also consider that population growth in the region is two times higher than the country's average (Garbossa et al., 2017) and the fact that the bays are economically important due to the summer tourism (~1.5 million visitors per year) and bivalve mollusks aquaculture (~70% of the Brazilian production) (Souza et al., 2017).

Here we examine, for the first time, how oceanographic and meteorological events affect the biogeochemical properties of the BSCI ecosystem, using a dataset covering the last three decades (1993–2019).

Besides the seasonal variability, we also investigated the fate and processes associated with nutrients and chlorophyll-a in the land-ocean interface, from the BSCI's main watersheds to the adjacent continental shelf. We hypothesize that i) the number of inhabitants in each sub-watershed is directly associated to water quality degradation, mainly during summer, due to the increase of tourism and precipitation; ii) new primary production and regeneration of organic matter are controlled seasonally by oceanic water masses and watershed runoff; and iii) El Niño and La Niña events modulate the trophic conditions in the watershed-bay-shelf continuum. Our approach was to apply multiple biogeochemical and eutrophication assessment tools in order to better understand the role of nutrient fluxes from the continental runoff and the oceanic water masses in the ecosystem metabolism. The goal of this study is to draw attention about the environmental issues of this region and support better coastal management strategies to restore and preserve this important ecosystem.

2. Material and methods

2.1. Study area

The BSCI is shaped by two water bodies, named as North and South Bay, which are connected in the middle by a narrow (~500 m) channel (Fig. 1). It is a well-mixed semi-enclosed system, where the waters are exchanged with the continental shelf in the extremes (Simonassi et al., 2010). The bay area and length are around 430 km² and 50 km, respectively. The drainage basin area is about 1875 km². The tidal regime is semi-diurnal, with measured daily amplitudes from 0.2 to 1.7 m (Garbossa et al., 2014). Tidal heights are lower than 1 m, but it can significantly increase during strong southerly winds events, concomitant with the spring tide. Local depths are less than 4 m in most of the bay, increasing up to 30 m in the central and south straits, where strong currents are observed (Silveira and Bonetti, 2019). Low-energy areas are found in the central region of the bay, due to the overlap of the tidal waves that came from both sides, generating a standing wave node (Garbossa et al., 2014).

2.2. Data acquisition

2.2.1. Water column

All available data, both new and already published, about the water quality of the watersheds, bays, and continental shelf were compiled in order to evaluate the spatial and seasonal variability (Table S1, Supplemental material). In all studies, depth, salinity, temperature and turbidity were acquired by sensors or multiparameter probes, previously calibrated. Dissolved oxygen (DO) concentration and saturation were measured by pre-calibrated sensors or by the Winkler method (Labasque et al., 2004). The apparent oxygen utilization (AOU) was calculated between the difference of the equilibrium saturation (depending on temperature, salinity, and pressure) and the in situ oxygen saturation (Benson and Krause, 1984). In all studies, water samples were collected to analyze the dissolved inorganic nutrients, chlorophyll-a and total suspended solids (TSS) by standard methods, using Van Dorn or Niskin bottles. The water samples were conditioned in previously acid-washed (HCl 10%) polyethylene bottles, cooled in a thermal box with ice, and kept in the dark until arrival in the laboratory.

The water was vacuum filtered in glass fiber filters of 0.45 or 0.7 µm of porosity and 47 mm of diameter for photosynthetic pigments and TSS analyses. Chlorophyll-a and pheophytin-a were

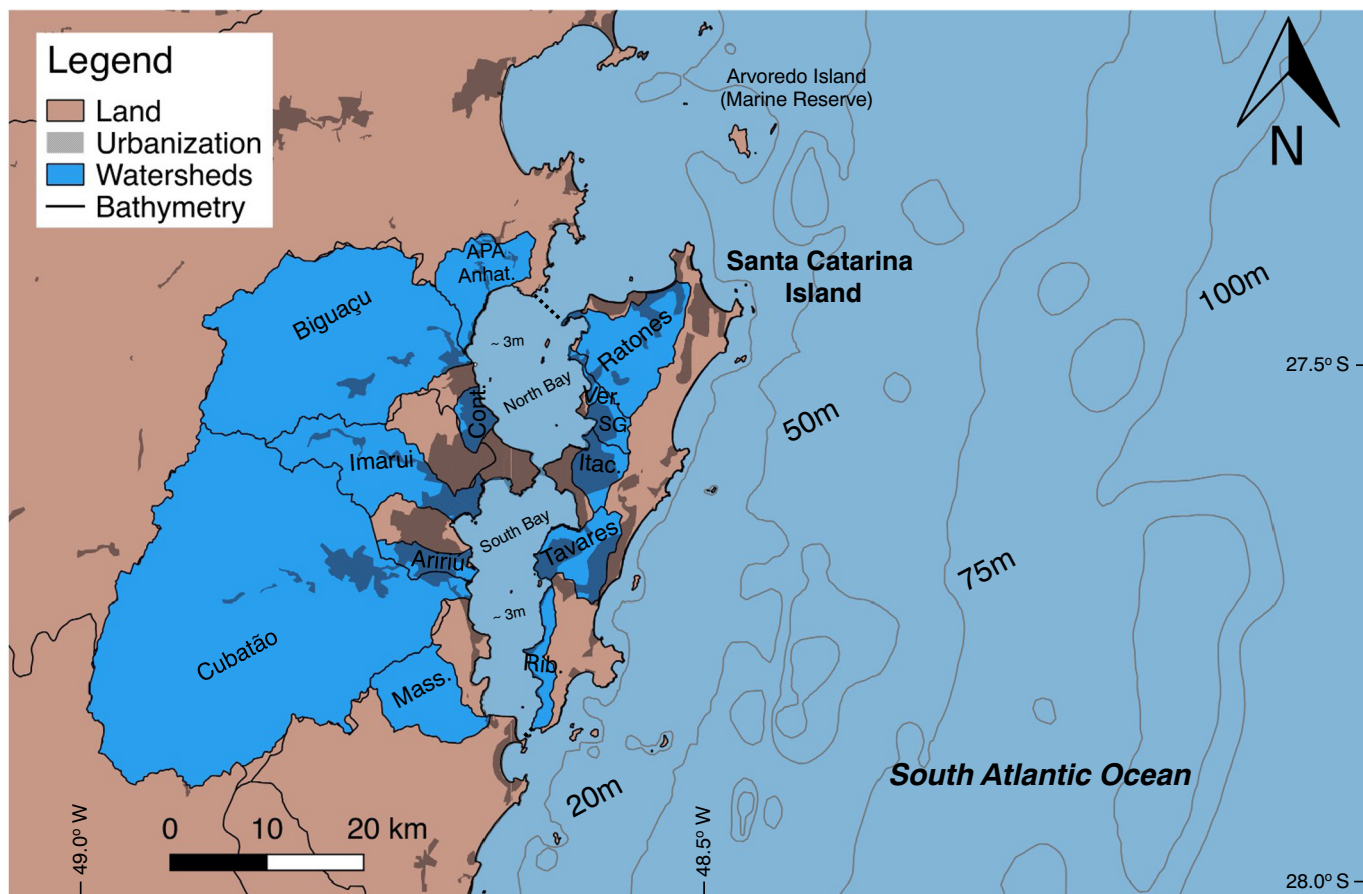


Fig. 1. Map of the watershed-bay-shelf continuum. The dotted lines in the extremes and the channel in the middle were defined as the limits among the North and South Bays and the continental shelf for modeling purposes. Watersheds: Mass. (Massiambú), Cubatão, Aririú, Imarui, Cont. (Continental), Biguaçu, APA Anhat. (Anatomirim), Rationes, Ver. (Veríssimo), SG (Saco Grande), Itac. (Itacorubi), Tavares and Rib. (Ribeirão).

determined spectrophotometrically, after 24 h of extraction with acetone, following Strickland and Parsons (1972). TSS was determined gravimetrically, by weighing the dry filters in analytical balances (Grasshoff et al., 1999). Nutrients (phosphate, nitrate+nitrite, ammonium+ammonia and silicate) were determined by the colorimetric method (Grasshoff et al., 1999), reading the absorbances in spectrophotometers. In order to check the quality of the reagents and equipment, standard curves were run daily prior to each nutrient analysis. Dissolved inorganic nitrogen (DIN) was calculated by sum nitrate+nitrite and ammonium+ammonia concentrations. It was assumed that phosphate is equal to the concentration of dissolved inorganic phosphorus (DIP). Ammonia (NH_3) and ammonium (NH_4^+) concentrations were determined as a function of pH, temperature and salinity (Bell et al., 2007; Whitfield, 1974). Fecal coliform data from 2002 to 2019 of the 16 sites inside the BSCI were provided by the State environmental agency (IMA-SC).

2.2.2. Meteorological variables

Daily meteorological data (temperature, precipitation, evaporation, and wind) from 1994 to 2019 were extracted of the National Institute of Meteorology (INMET-Brazil) historical database. The meteorological station (N° 83897) is located in the South Bay margin, 5 m above the ground. The multivariate ENSO index (MEI) is a method to identify the frequency and intensity of the El Niño Southern Oscillation in both phases, La Niña (negative) and El Niño (positive) (Wolter and Timlin, 2011). The index fluctuates from -3 to 3 , categorizing the ENSO events as weak ($0.5-1$), moderate ($1-1.5$), strong ($1.5-2$) and very strong (>2), positive values refers to El Niño and negative to La Niña. The

data were extracted from the website <https://www.esrl.noaa.gov/psd/enso/mei/>, in order to give an index for each day of sampling.

2.3. Land-ocean interactions in the coastal zone (LOICZ) biogeochemical model

The LOICZ model uses a biogeochemical mass-balance approach to quantify water and nutrient fluxes and to estimate the metabolism of estuarine systems (Gordon et al., 1996; Swaney et al., 2011). In this study, we modeled the South and North Bay separately, since sampling in those sites were made mostly in different days. Daily averages of salinity and nutrients from multiple sampling points of each bay were used to build a single box, following LOICZ guidelines (Gordon et al., 1996). In the North Bay, 46 days were selected from 2005 to 2018. In the South Bay, we compiled a larger dataset (86 days), from 1996 to 2017. Salinity and nutrient data from the continental shelf and the main rivers were retrieved from our database. Meteorological data (precipitation and evaporation) were acquired from a nearby meteorological station, as described in Section 2.2.2. DIN and DIP concentration in the rain were obtained from Hoinaski et al. (2014) and Mizerkowski et al. (2012), respectively. Daily freshwater runoff of BSCI main watersheds ($N = 13$) was calculated following LOICZ guidelines (Dupra et al., 2000) and calibrated with in situ water flow measurements (Garbossa et al., 2017). Non-conservative budgets (Δ_{DIN} and Δ_{DIP}) were calculated considering the rivers (V_Q), precipitation (V_P), residual (V_R) and oceanic (V_X) fluxes as sources and sinks of nutrients between the bays and the continental shelf. The net ecosystem metabolism (NEM), phytoplankton primary production minus mineralization ($p - r$), and the relative importance of N fixation or

denitrification ($N_{\text{FIX-D}}$) were calculated through CNP (carbon, nitrogen and phosphorus) Redfield stoichiometry (Swaney et al., 2011).

2.4. Eutrophication assessment methods

2.4.1. Assessment of estuarine trophic status (ASSETS)

The ASSETS method was designed to evaluate the susceptibility to eutrophication of coastal ecosystems by the influencing factors-IF (pressure), eutrophic conditions-EuC (state) and future outlook-FO (response) (Bricker et al., 2003). Those three parameters are used to calculate the overall assessment or level of expression, which is given by a trophic status classification: bad (worsen), poor, moderate, good and high (better). All the calculations were made in the ASSETS software (<http://www.eutro.org>), following the recommendations of Ferreira et al. (2007). We used the coastal bay equations, considering the seawater zone indicated by the model (salinity >25). Physical parameters, such as mean tidal prism and tidal range, were obtained from Garbossa et al. (2017). We generated a model for each bay (North and South) separately, during the 1990's, 2000's and 2010's.

The decadal medians of DIN concentration in the main rivers and continental shelf were obtained from our dataset. Nitrogen load decadal medians of the rivers were estimated by the LOICZ model (VQ_{DIN}). Chlorophyll-a and DO were calculated by 90th and 10th decadal percentile, respectively, as recommended by Ferreira et al. (2007). Toxic bloom duration and frequency were obtained from the Santa Catarina farming development company (CIDASC). The future scenarios were estimated for the next decade (2020–2030), considering the system's natural susceptibility to eutrophication (e.g. flushing time and N loads) and foreseeable changes in the land-uses and effluent treatment. We considered that agriculture and urbanization correspond to 20% and 80% of BSCI land-uses. Also, that population will increase up to 25% and agriculture will stay the same, following the municipalities' directive plan. We simulated effluent treatment as it is now, around 27% of the urban area (Garbossa et al., 2017), and with 100% of population served by the sewerage system.

2.4.2. Trophic index (TRIX)

The trophic index TRIX is used to characterize the trophic status of coastal waters, by the linear relation of chlorophyll-a ($\text{mg}\cdot\text{m}^{-3}$), DIN ($\text{mg}\cdot\text{m}^{-3}$), DIP ($\text{mg}\cdot\text{m}^{-3}$) and the absolute percentage of deviation (100%) from oxygen saturation values (aD\%DO) (Vollenweider et al., 1998). The index covers a spectrum of 5 trophic conditions: ultra-oligotrophic (0–2), oligotrophic (2–4), mesotrophic (4–6), eutrophic (6–8), and hypertrophic (8–10) (Giovanardi and Vollenweider, 2004). The index is also used to classify the water quality in 4 categories: elevated (<4), good (4–5), poor/mediocre (5–6) and bad (>6) (Rinaldi

and Giovanardi, 2011). An index was calculated for each sample of BSCI ($N = 590$) and the watersheds ($N = 365$), following Eq. (1). Where “k” is the sum of the minimum logarithmic value of each variable (ΣLogMin) and “m” is the scale factor [$(\Sigma\text{LogMax} - \Sigma\text{LogMin}) \cdot (0.1)$]. The TRIX formula was calibrated for both the bay ($k = -1.49$; $m = 1.31$) and the rivers ($k = -1.00$; $m = 1.00$).

$$\text{TRIX} = \left[\frac{\text{Log10}(\text{Chlorophyll-a} * \text{DIN} * \text{DIP} * \text{aD\%DO}) - k}{m} \right] \quad (1)$$

2.5. Statistical analyses

The boxplot graphs and correlation analyses were performed using the RStudio software (R Core Team, 2015). Kruskal-Wallis (KW) test was applied to verify significant ($p < 0.05$) univariate differences between groups. When KW was significant, the Dunn's post-hoc test was used to obtain pairwise comparison results. The p values were adjusted with the Bonferroni method. Principal coordinates analysis (PCO) was used to explore spatio-temporal variability and its main indicators. Samples were previously transformed by $\log(x + 1)$. The resemblance matrix was calculated by the Gower coefficient. The permutational multivariate analysis of variance (PERMANOVA) was applied in the same resemblance matrix used in the PCOs to verify significant differences ($p < 0.001$) among the groups (classified by seasonal and/or spatial factors).

PCO and PERMANOVA were performed in the PRIMER-E software (Anderson, 2017; Clarke and Warwick, 2001). Mann-Kendall tests in the “R” package ‘wq’ were used to verify if the temporal trends were significant ($p < 0.05$) (Harding et al., 2019). The generalized additive model (GAM) was used to verify which variables better explain chlorophyll-a variability in the bays. The dataset was standardized before GAM analysis. The GAM was performed in the RStudio software using the “gam” and “mgcv” packages, AIC model, “tw” family and the gaussian function (R Core Team, 2015). The Ocean Data View (ODV) software was used to plot the water masses over the continental shelf of South Bay.

3. Results

3.1. Spatial variability pattern across the watershed-bay-shelf continuum

The rivers showed the highest concentrations of nutrients and lowest levels of DO among all the systems (Table 1). The first component of Fig. 2 (PCO 1) corresponds to the largest variance in the dataset, where the position of samples in the ordination space was found to reflect the environmental gradient over the watershed-bay-shelf continuum. The contribution of each variable to sample dispersion along the axes was

Table 1
Median, minimum and maximum values of the biogeochemical variables across the watershed-bay-shelf continuum, considering all the dataset. Freshwater (Salinity <0.5), Estuarine Zone (0.5 < Salinity <30) and Seawater (Salinity >30). When significant ($p < 0.05$), super-script letters indicate the Kruskal-Wallis pairwise comparison test results, where $A > B > C > D > E$.

System	Rivers	Rivers	Bay	Bay	Shelf
Salinity zone	Freshwater ($N = 155$)	Estuarine zone ($N = 522$)	Estuarine zone ($N = 371$)	Seawater ($N = 1320$)	Seawater ($N = 649$)
pH	7.0 (5.5–8.4) ^C	7.4 (5.8–11.0) ^B	8.2 (6.7–8.8) ^A	8.1 (6.1–9.9) ^A	8.2 (6.1–8.9) ^A
DO ($\text{mg}\cdot\text{L}^{-1}$)	4.4 (0.0–11.5) ^C	4.4 (0.0–12.4) ^C	7.1 (4.3–10.9) ^A	6.8 (1.8–11.4) ^B	6.7 (1.6–11.5) ^B
DIP ($\mu\text{mol}\cdot\text{L}^{-1}$)	1.9 (0.1–159.4) ^A	0.9 (0.1–123.2) ^A	0.4 (0.1–5.9) ^B	0.5 (0.1–6.5) ^B	0.4 (0.1–2.1) ^B
Ammonium ($\mu\text{mol}\cdot\text{L}^{-1}$)	40.4 (0.4–284.5) ^A	9.0 (0.1–256.8) ^B	4.7 (0.3–108.0) ^C	3.1 (0.2–85.2) ^C	1.3 (0.1–13.5) ^D
Nitrate ($\mu\text{mol}\cdot\text{L}^{-1}$)	12.8 (0.3–123.4) ^A	3.9 (0.1–77.3) ^B	2.1 (0.1–9.3) ^C	1.3 (0.1–10.0) ^D	1.0 (0.1–8.6) ^E
NP Ratio	26.5 (0.1–1402.0) ^A	14.0 (0.1–336.0) ^B	14.7 (0.3–691.0) ^B	8.2 (0.1–999.1) ^C	5.9 (0.6–770.9) ^D
Silicate ($\mu\text{mol}\cdot\text{L}^{-1}$)	89.3 (0.4–365.2) ^A	57.0 (0.4–720.8) ^A	19.5 (2.2–106.3) ^B	14.2 (0.2–144.5) ^C	7.4 (0.3–42.7) ^D
Chlorophyll-a ($\mu\text{g}\cdot\text{L}^{-1}$)	1.8 (0.1–197.8) ^B	4.8 (0.1–180.9) ^A	3.0 (0.2–66.1) ^A	3.1 (0.1–68.5) ^A	1.6 (0.1–79.2) ^B
Pheophytin-a ($\mu\text{g}\cdot\text{L}^{-1}$)	0.1 (0.1–77.0) ^B	17.5 (0.1–176.0) ^A	9.7 (0.1–96.6) ^A	5.6 (0.1–80.9) ^A	0.7 (0.1–70.9) ^B
TSS ($\text{mg}\cdot\text{L}^{-1}$)	15.4 (0.7–899.6) ^B	36.0 (0.3–490.2) ^A	27.0 (0.3–1498.2) ^A	20.0 (0.1–1078.6) ^B	17.5 (1.3–1094.1) ^B

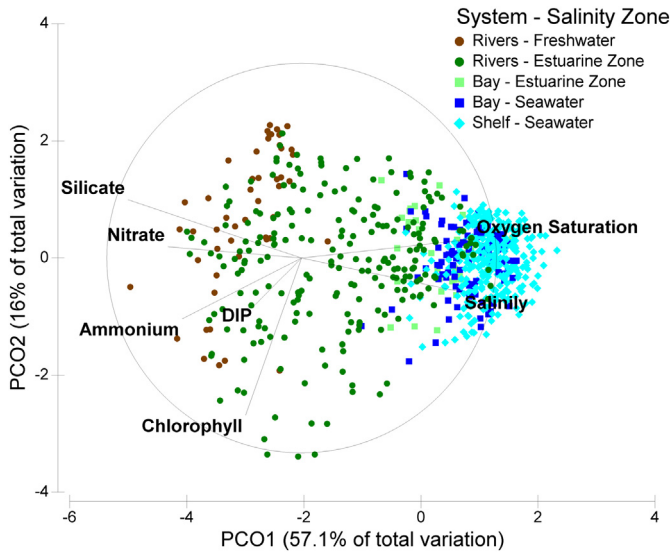


Fig. 2. Principal coordinates analysis (PCO) emphasizing the biogeochemical pattern across the watershed-bay-shelf continuum ($N = 715$). Freshwater (Salinity <0.5), Estuarine Zone ($0.5 < \text{Salinity} < 30$) and Seawater (Salinity >30). The plot shows the distance among samples (colored symbols) and variables scores (arrows) for the first two components of PCO.

estimated from correlation analysis. The main descriptors of PCO1 were salinity ($r = 0.59$), silicate ($r = -0.50$) and ammonium ($r = 0.42$) (Fig. 2). These associations are represented in Fig. 2 by the length (the larger, the stronger the relationship) and by the direction (positive and negative correlation) of the vectors. The main descriptor of PCO2 was chlorophyll-a ($r = -0.76$), indicating that the highest

phytoplankton biomass was found in the estuarine zone of the rivers, concomitantly with the pheophytin-a and TSS peaks (Table 1).

The NP ratio indicated that the system was limited by P in the freshwater domain and by N in the seawater zone (Table 1). The PERMANOVA, applied on the same dataset used to perform the PCO (salinity, oxygen saturation, chlorophyll-a, ammonium, DIP, nitrate and silicate) (Table S2), indicated that all the systems are significantly ($p < 0.05$) different from each other, strong dissimilarities were observed between the shelf and rivers and slight differences between the bay systems and the rivers (estuarine zone) and shelf waters. Ammonium was the main nutrient in the DIN pool, both in the North Bay ($62 \pm 29\%$), South Bay ($74 \pm 24\%$), continental shelf ($56 \pm 23\%$) and rivers ($63 \pm 32\%$). Ammonia contributed with only $0.2 \pm 0.8\%$ of the total DIN, but concentrations were found up to $7.7 \mu\text{M}$ in the rivers. Watershed population was associated with high DIN, chlorophyll-a, coliform and TRIX (Fig. 3). Also, in the rivers, Secchi disk depth was highly correlated with TRIX ($r = -0.97$; $p < 0.05$).

3.2. Seasonal variability

3.2.1. Rivers

In the rivers, salinity and DO were significantly higher ($p < 0.05$) in the winter, compared to summer, while temperature, DIN, fecal coliform and turbidity were lower ($p < 0.05$) in winter than summer, as indicated by Kruskal-Wallis tests (Fig. 4). DIP did not show a clear pattern through the seasons of the year (Fig. 4e). Chlorophyll and turbidity showed an inverse correlation ($r = -0.32$, $p < 0.05$). Considering the Brazilian water quality legislation (CONAMA 357/2005), samples in disagreement with regulations were found in all seasons. Water quality showed a slight improvement in the winter, mainly for DO, DIN and coliform (Fig. 4). Oxygen concentrations were below the CONAMA legislation in 27% of the samples during winter, whereas 66% of the samples

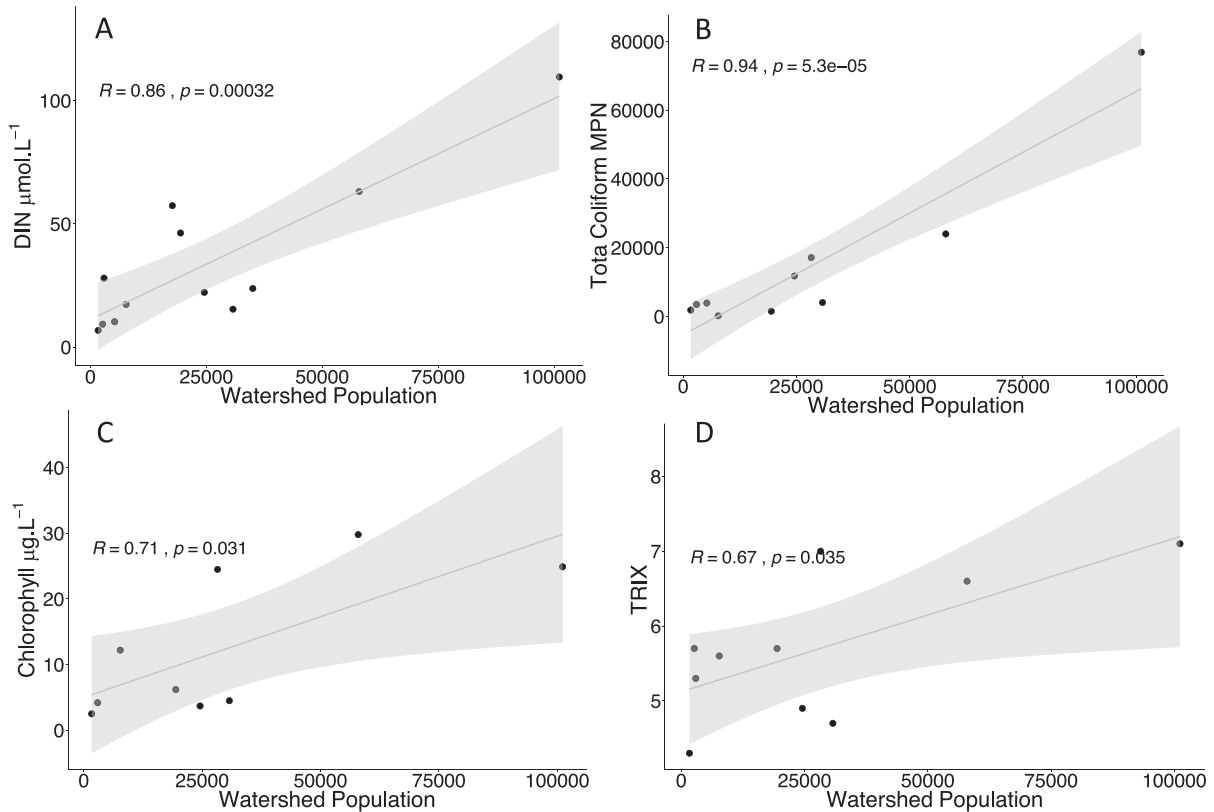


Fig. 3. Scatter plot between a) DIN (dissolved inorganic nitrogen), b) total coliform (MPN – most probable number in 100 mL^{-1}), c) chlorophyll-a and d) TRIX vs the number of inhabitants of the BSCI main sub-watersheds. Pearson correlation algorithm was used to obtain the p and R values. The grey lines indicate 95% confidence intervals.

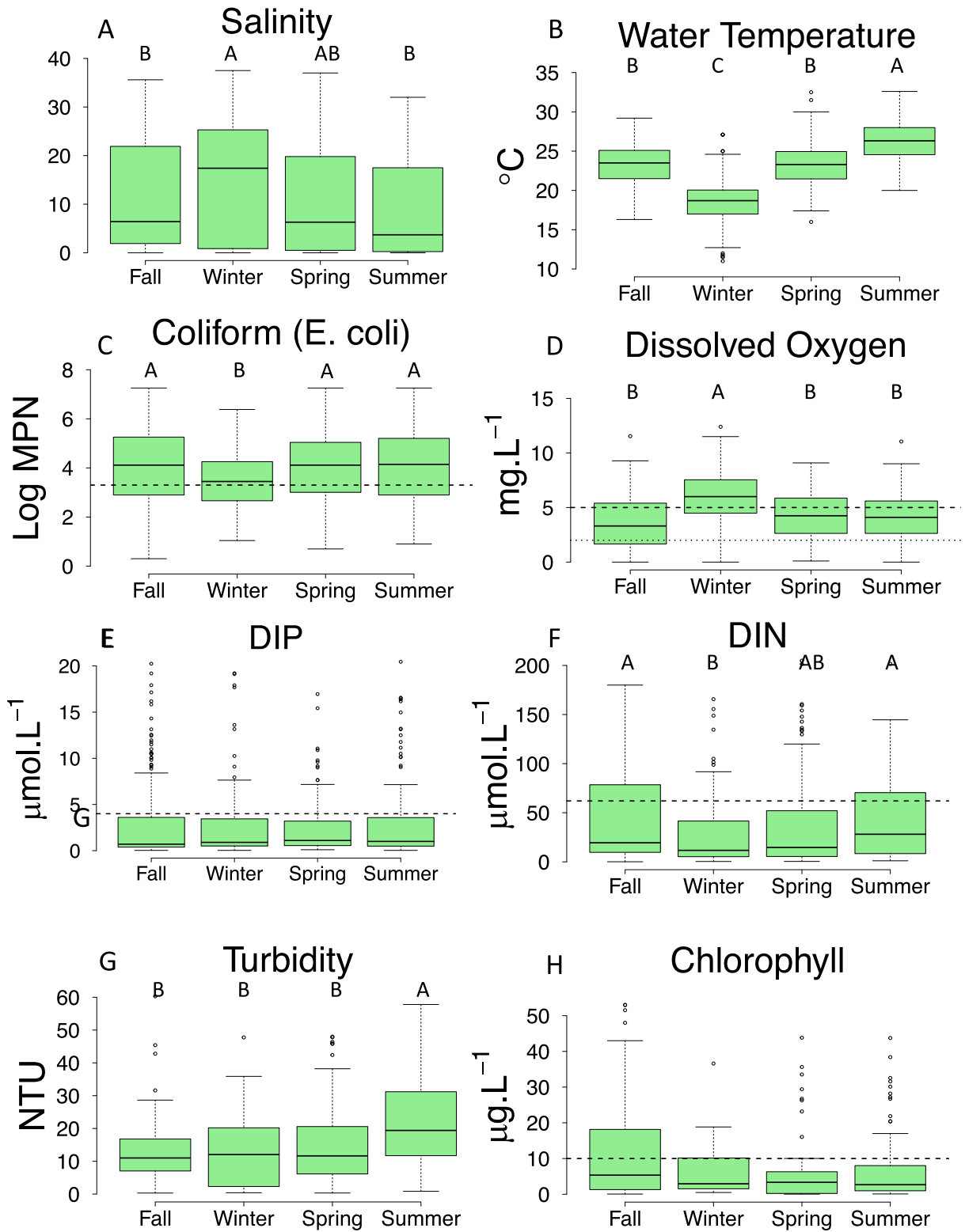


Fig. 4. Boxplot (minimum, maximum, median, first quartile, third quartile, and outliers) of the physical and biogeochemical properties of all main watersheds ($N = 13$) of BSCI by the seasons of the year. The dashed line indicates the maximum (Coliform, DIP, DIN, and Chlorophyll-a) and minimum (Dissolved Oxygen) thresholds according to the Brazilian water quality legislation (CONAMA 357/2005) for estuarine waters. The dotted line (Fig. 4d) indicates the threshold for hypoxia (2.0 mg.L^{-1}). Salinity ($N = 676$), Water Temperature ($N = 675$), Fecal Coliform ($N = 1146$), Dissolved Oxygen ($N = 623$), DIP (Dissolved Inorganic Phosphorus, $N = 610$), DIN (Dissolved Inorganic Nitrogen, $N = 616$), Turbidity ($N = 298$) and Chlorophyll-a ($N = 369$). When significant ($p < 0.05$), upper-case letters indicate the Kruskal-Wallis pairwise comparison test results, where $A > B > C$.

were below limits in the other seasons. Hypoxic conditions ($< 2.0 \text{ mg.L}^{-1}$) were found in 20% of the cases, especially in fall. Coliform concentrations were above limits (2000 MPN/100 mL) in 43% of samples

during winter against 66% during the other seasons. As for chlorophyll-a, 28% of the samples were above limits, mainly during fall. DIP and DIN were both above limits in 25% of the samples.

3.2.2. Bays and continental shelf

The water column seasonality of BSCI was driven mainly by temperature, as indicated by its strong correlation ($r = -0.99$) with axis 1 of PCO (Fig. 5). The spatial distribution was driven by salinity, positively correlated ($r = 0.80$) with axis 2. In the negative side of both axes of PCO (Fig. 5), high DIN and chlorophyll-a values were concentrated in the samples inside the bays in the spring-summer seasons and also some samples of South Bay during winter (Fig. 5). Whereas, the lowest concentrations of nutrients and chlorophyll-a were observed in the continental shelf during all seasons (positive side of axis 2). Considering the same dataset used in the Fig. 5, the PERMANOVA showed that the differences between regions are dependent on the seasonality (Table S3). When the seasons were analyzed separately, there were no significant differences ($p = 0.054$) between the North and South bays during the spring-summer (Table S2). In the winter-fall, however, the South and North bays showed significant ($p < 0.05$) differences. Moreover, the continental shelf and the bays were significantly different ($p < 0.05$) during all seasons (Table S2). Three water masses were identified over the continental shelf of South Bay, both in the fall and winter seasons (Fig. 6). A strong influence of continental plumes over the shelf was observed in both seasons; the South Bay plume in the fall and the Plata Plume Water (PPW) in the winter (Fig. 6).

Considering the LOICZ results, the residence times (WRT) observed in the winter were 6 and 3 times higher than in the summer in the North and South bay, respectively (Table 2). WRT was inversely correlated ($p < 0.05$) with rain ($r = -0.77$) and water temperature ($r = -0.72$), while pheophytin-a ($r = 0.66$) and apparent oxygen utilization ($r = 0.52$) showed positive correlation with WRT. Residual (VR) and riverine (VQ) nutrient fluxes were higher in the summer than winter, both for DIP and DIN. P exchanges with the continental shelf (VX) were more important in the South Bay, while the N flux was more important in the North Bay. The riverine nutrient inputs (VQ) were the main nutrient source for the bays (Table 2). The North Bay exported 4.5% and 12.4% of all N and P inputs to the continental shelf, respectively (Table 2). In the South Bay, 5.6% of N and 21.9% of P were exported. Both systems behaved as a sink of nutrients most of the time, shifting to

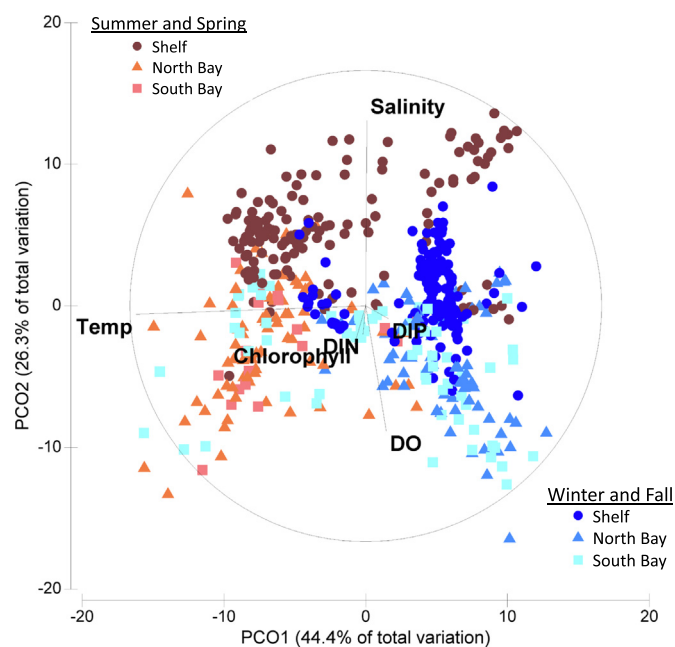


Fig. 5. Principal coordinate analysis (PCO) emphasizing the seasonal and spatial variability of Temperature (Temp), Salinity, Dissolved Oxygen (DO), DIP, DIN and chlorophyll-a in the bays and continental shelf ($N = 584$).

sources of P and N during winter in the North and South bays, respectively (Table 2). Autotrophic conditions prevail in 63% of the sampled days in both systems throughout the year. Heterotrophic metabolism or near balance was mostly observed in the winter. The NEM (Net Ecosystem Metabolism, as production - respiration) was correlated ($p < 0.05$) to rain ($r = 0.88$), WRT ($r = -0.71$) and TRIX ($r = -0.51$). The LOICZ model indicates that denitrification predominates over N fixation in the North Bay (Table 2), removing about 60% of all N inputs and limiting primary productivity. N fixation predominates in the South Bay (Table 2), where about 13% of all DIN came from this process.

3.3. Interannual, decadal and El Niño-Southern Oscillations

The NP ratio is decreasing over the years in the BSCI, shifting the system from P to N limiting (Fig. 7b). Considering the Mann-Kendall trend tests, DIP and TSS increased, whereas DIN and silicate are decreasing over time (Fig. 7). The trophic index oscillated between mesotrophic (4–6) and eutrophic (6–8) (Fig. 7f). Giving the importance of chlorophyll-a as a predictor of harmful algal blooms, a generalized additive model (GAM) was applied in order to better understand its behavior and main descriptors (Table 3). The model showed that ENSO events and temperature have strong control over chlorophyll-a concentrations, followed by salinity, DO and year sampled. Although the partial correlations were statistically significant ($p < 0.05$), the model showed low predictivity (14.9%), suggesting that other drivers are important to explain chlorophyll-a variation in the bays.

El Niño events increased precipitation rates (Fig. 8) and affected the bays and continental shelf in different ways. In the bays, there was a tendency to lower nutrients and chlorophyll-a during El Niño, whereas the opposite was observed in the continental shelf (Fig. 9). This pattern seems to reverse during La Niña (Fig. 9). However, both systems showed high AOU and low salinity during El Niño events (Fig. 10). Chlorophyll-a was correlated ($p < 0.05$) with the MEI in the bays ($r = -0.49$) and shelf ($r = 0.54$).

The ASSETS model overall grade showed poor and bad trophic status for the North and South bay, respectively, which agreed with other methodologies (TRIX and LOICZ) (Table 4). Considering the influencing factors (IF) to natural susceptibility to eutrophication (e.g. nutrient dilution and flushing potential), the systems showed moderate-high to high pressure. As for the eutrophic conditions (EuC), moderate-high state was observed, except in the South Bay during the 2010's, mostly due to the increase of 90th percentile of chlorophyll-a (primary symptom) from $5.3 \mu\text{g.L}^{-1}$ in the 1990's to 6.8 in the 2000's and 8.9 in the 2010's. The 10th percentile of DO (secondary eutrophication symptom) indicated biological stressful conditions ($<5 \text{ mg.L}^{-1}$) just in the North Bay in the 2010's. The analysis of the future outlook (FO) showed that the susceptibility to eutrophication will likely remain the same, considering three different scenarios and the assumptions detailed on Section 2.4.1 (Table 4).

4. Discussion

4.1. Anthropogenic pressures

The BSCI is under moderate to high eutrophication pressure due to the poor regulations and enforcement of land-uses, especially those related to urban planning and sanitation. Disposal of effluents from rural activities or untreated domestic and industrial sewage is a generalized problem in the estuaries of South America (Barletta et al., 2019). BSCI is no exception, although there are wastewater treatment plants (WWTPs) in some watersheds, they are not enough to prevent the input of pollutants. The WWTPs covers primary and secondary treatment only, which removes just up to 20–50% of nutrients, increasing the susceptibility to eutrophication (Carbossa et al., 2017). Furthermore, just about 27% of the households have access to

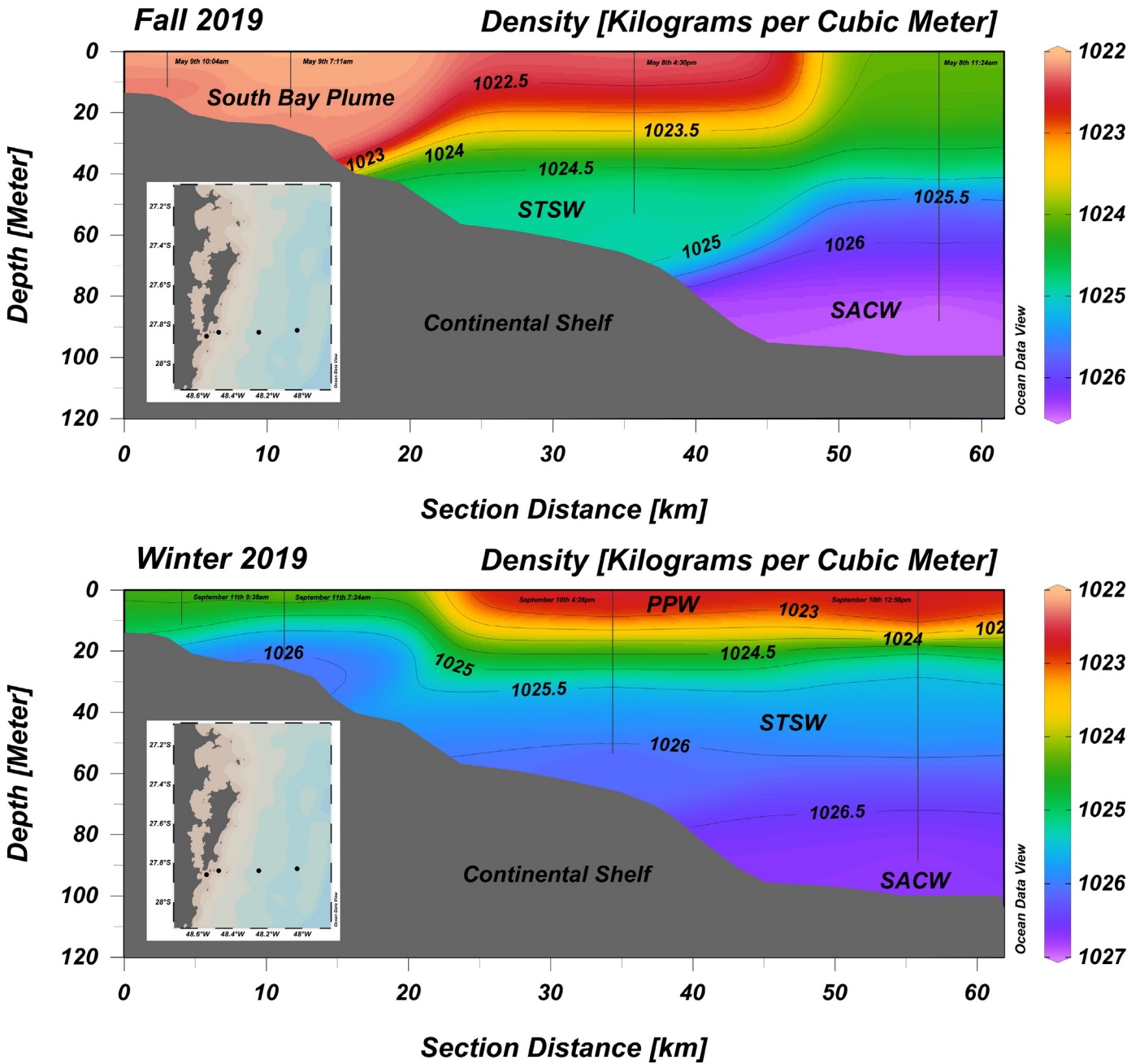


Fig. 6. Water mass seasonality over the continental shelf of South Bay in the fall (May 8-9th) and winter (September 10-11th) of 2019. The vertical and horizontal lines indicate the CTD profiles and isopycnals, respectively. The STSW (Subtropical Shelf Water), SACW (South Atlantic Central Water) and PPW (Plata Plume Water) water masses were characterized according to Möller et al. (2008).

Table 2
Median of the water residence time (WRT, days), DIP and DIN budgets ($10^3 \cdot \text{mol} \cdot \text{day}^{-1}$), Net Ecosystem Metabolism (NEM, production - respiration, $\text{gC} \cdot \text{m}^{-2} \cdot \text{day}^{-1}$) and the relative importance of N fixation and denitrification ($N_{\text{FIX}} - D$, $\text{mmolN} \cdot \text{m}^{-2} \cdot \text{day}^{-1}$) for the North (2005–2018) and South (1996–2017) bays during the seasons of the year. VR (nutrient residual flux), VX (nutrient oceanic flux), VQ (watershed nutrient flux) and Δ (nutrient internal production - consumption).

Region	Season	WRT	VRDIP	VXDIP	VQDIP	Δ DIP	NEM	VRDIN	VXDIN	VQDIN	Δ DIN	$N_{\text{FIX}} - D$
North Bay	Fall	34.73	-0.05	-0.25	0.94	-0.76	0.06	-0.33	0.14	7.42	-10.06	0.02
	Winter	55.96	-0.12	-1.08	1.13	0.27	-0.02	-0.59	-0.15	9.00	-8.85	-0.11
	Spring	32.62	-0.45	-4.07	3.33	-0.20	0.02	-2.64	25.50	26.43	-67.85	-0.67
	Summer	9.27	-1.10	-1.12	6.33	-1.55	0.13	-8.70	10.42	50.19	-47.97	-0.12
South Bay	System	26.34	-0.55	-1.27	3.35	-0.78	0.07	-2.79	6.14	26.53	-27.04	-0.13
	Fall	11.28	-1.39	2.46	2.00	-3.76	0.31	-6.71	-143.56	146.14	-7.69	0.67
	Winter	27.53	-0.10	-0.22	0.28	0.02	-0.01	-1.02	-81.49	20.41	29.59	0.05
	Spring	9.90	-0.90	-0.01	1.57	-0.76	0.06	-14.34	-129.24	113.13	1.88	0.50
	Summer	8.81	-2.02	2.20	2.11	-3.62	0.30	-10.57	-99.75	153.86	-6.09	-0.06
System	14.92	-0.88	0.36	1.34	-1.09	0.09	-8.35	-97.94	97.63	10.52	0.19	

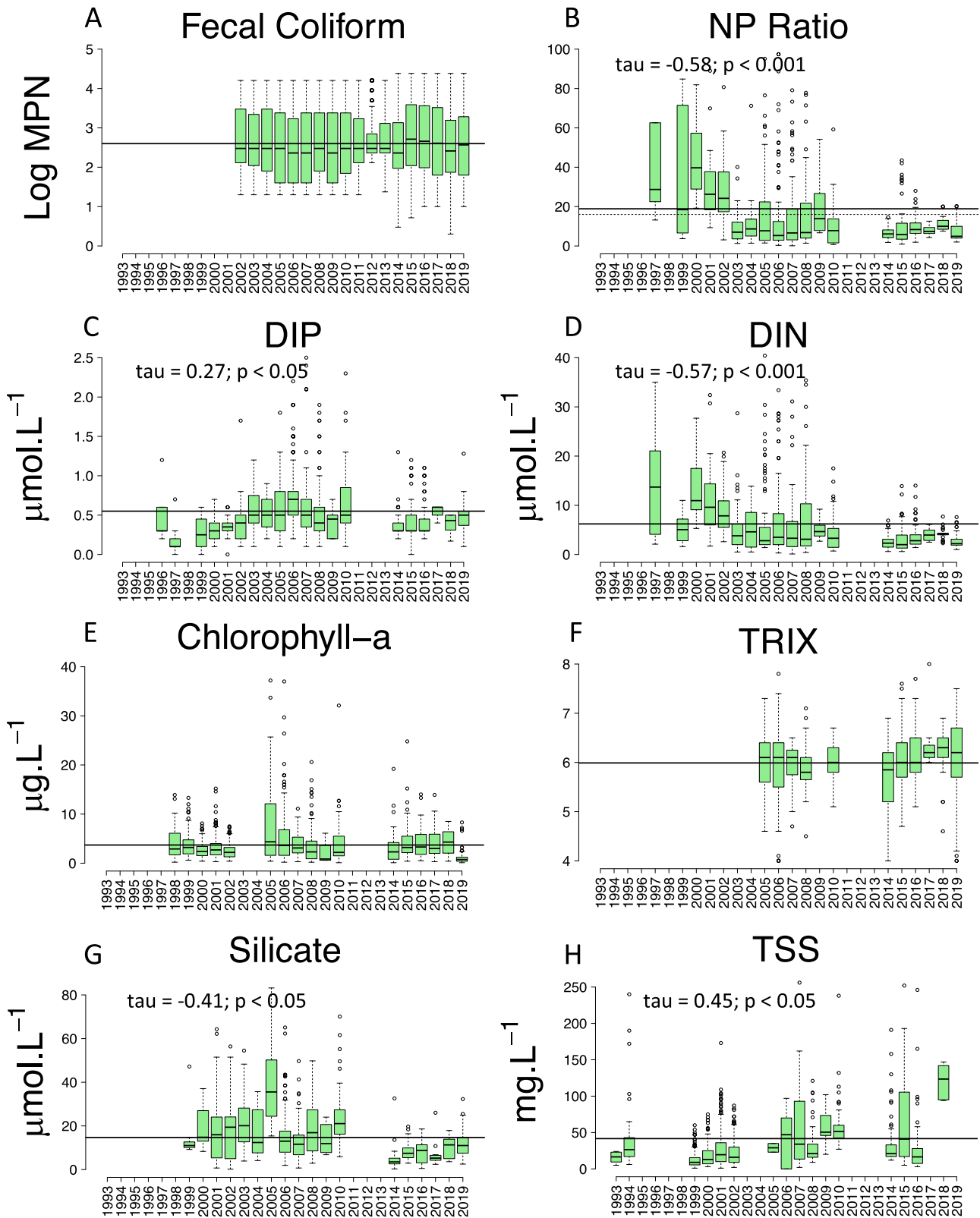


Fig. 7. Long-term time-series boxplot (minimum, maximum, median, first quartile, third quartile, and outliers) for the Fecal Coliform ($N = 8084$), NP Ratio ($N = 1034$), DIP ($N = 1193$), DIN ($N = 1152$), Chlorophyll-a ($N = 1748$), TRIX ($N = 653$), Silicate ($N = 878$) and TSS - Total Suspended Solids ($N = 1565$) in the BSL. The line represents the historical average of each variable. The dashed line indicates the Redfield ratio (16N:1P) in the Fig. 7b. Mann-Kendall tests are shown by the strength of association (τ) for significant trends ($p < 0.05$).

sewerage, while most of the population uses cesspool tanks or dumps raw sewage into the small streams that drain to the bays. Risks of waterborne diseases have been associated with water

quality degradation and elevated trophic status, mainly in the watersheds in the north of the island, where the rivers and groundwater are used as source of freshwater (Silva and Fonseca, 2016).

Table 3

Generalized additive model (GAM) results for the bays between 1993 and 2019 ($N = 349$ days). Chlorophyll-a as the dependent variable and the MEI (multivariate ENSO index), water temperature, salinity, DO (dissolved oxygen) and year as predictors. R^2 (adjusted) = 0.14, Deviance explained = 14.9%, GCV = 0.34, and Scale est. = 0.34.

Chlorophyll-a	Estimate	Std. error	t value	p value	ANOVA	
(Intercept)	-333.9	147.3	-2.3	0.024000	F value	p value
MEI	-0.9	0.2	-4.4	0.000017	19.0	0.00002
Temperature	0.9	0.2	4.6	0.000007	18.7	0.00002
Salinity	-2.3	0.5	-4.8	0.000003	13.4	0.00029
DO	0.4	0.2	2.0	0.049400	5.6	0.01807
Year	44.8	19.4	2.3	0.021500	4.3	0.03888

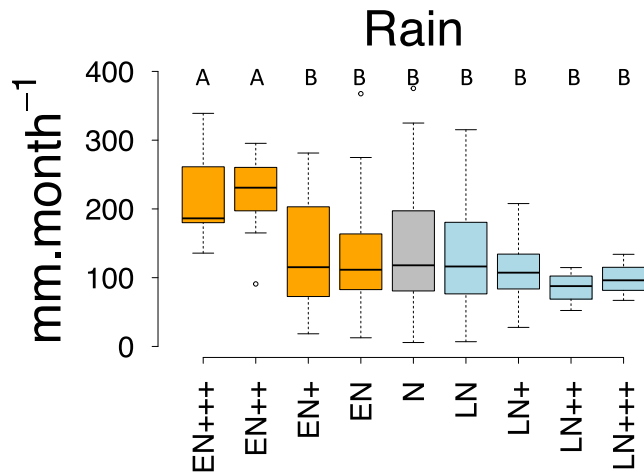


Fig. 8. Boxplot (minimum, maximum, median, first quartile, third quartile, and outliers) of accumulated monthly precipitation across ENSO events. EN (El Niño, orange), N (Neutral, grey) and LN (La Niña, blue). The signals represent the intensity, according to the Multivariate ENSO Index (MEI): +++ (very strong, $MEI > 2$), ++ (strong, $1.5 < MEI < 2$), + (moderate, $1 < MEI < 1.5$) and no signal (weak, $0.5 < MEI < 1$). All the sampled days with MEI between -0.5 and 0.5 were classified as neutral phase (N). When significant ($p < 0.05$), upper-case letters indicate the Kruskal-Wallis pairwise comparison test results, where $A > B$. (For interpretation of the references to colour in this figure legend, the reader is referred to the web version of this article.)

This study demonstrates that the number of inhabitants of each sub-watershed of BSCI is directly correlated to the increase of nitrogen, chlorophyll-a, and coliforms in the water column, also increasing the trophic state from mesotrophic to eutrophic. Our data also showed that the impact is extended to the estuarine and seawater zones. For example, even though the worst-case scenarios were found in the rivers, high nutrient concentrations were measured in the surface waters of the South Bay outfall (ETE Insular) in the winter of 2012, where DIP ($5.3 \mu\text{M}$) was above the regulations ($4.0 \mu\text{M}$), indicating sewage contamination. High DIP ($1.0 \mu\text{M}$) and DIN ($22.7 \mu\text{M}$) were also measured ~ 1 km away from the outfall, almost two and three times the long-term mean concentration found in the bay's estuarine waters, respectively. The content of organic matter ($14.0 \pm 1.2\%$) and carbon ($3.1 \pm 0.9\%$) in the sediment (this study) next to the outfall was also above the average values found in the South Bay, of 2.5% and 1.1% (Sewald et al., 2012; Vianna and Bonetti, 2018), respectively. This indicates that the WWTPs technology and coverage needs improvement in order to better manage the eutrophication problem.

Several studies have stated that aquaculture activities can significantly damage the water quality and biodiversity of coastal ecosystems, although other studies indicated that shellfish culture can help to reduce eutrophication by removing chlorophyll and increasing water transparency (Silva et al., 2011; Zimmer-Faust et al., 2018). In the

BSCI, bivalve aquaculture might be suppressing phytoplankton growth, keeping concentrations below $10 \mu\text{g.L}^{-1}$ most of the time, although eutrophication risk is still high due to periodic harmful algal blooms and continuous sewage inputs. In other systems, such as the San Francisco Bay, the introduction of a non-native species of clam (*Potamocorbula amurensis*) is reported to be the main cause of phytoplankton biomass loss due to the rapid grazing pressure (Cloern, 2019). In the BSCI, aquaculture farms were established in the 1980's, introducing the Pacific oyster *Crassostrea gigas* and the brown mussel *Perna perna*. Nowadays, the region produces up to $21,000 \text{ ton}\cdot\text{year}^{-1}$, encompassing about 70% of all bivalve aquaculture produced in Brazil (Netto et al., 2018). There is no chlorophyll-a data before the implementation of aquaculture in the region, but filter feeders might be controlling phytoplankton biomass, although other factors, such as nitrogen limitation and turbidity may be influencing as well.

Despite the importance of aquaculture, tourism also has a major role in the economy of Santa Catarina Island, mainly in the summer. In this season, most of the beaches inside the bays are in non-compliance with regulations for swimming and other recreational uses, due to high fecal coliform concentrations. Also, the pressure over the WWTPs increases during summer, when population rises up to 208% in some watersheds and rainfall events overload their capacity (Silva et al., 2016). However, beaches are not closed when coliform threshold is exceeded, although the State environmental agency puts signs warning that the waters are inappropriate for recreation and fishing, no further action is taken.

Fecal coliforms are associated with other pathogens that can concentrate in the shellfish tissues, favoring the risks of food poisoning since they are frequently eaten raw (Zimmer-Faust et al., 2018). In the BSCI, 54% of the samples showed proper conditions for swimming, considering all the time series (2002–2019) and the 16 sites monitored in the bays by the State environmental agency (IMA-SC). However, since the system is used by shellfish farms, there is a more restrictive legislation (CONAMA 274/2000), that, when applied, indicates that only 26% of the samples were suitable for bivalve aquaculture. In the rivers, just 36% of the samples agreed with the legislation for swimming and other recreational uses ($<2000 \text{ MPN}/100 \text{ mL}$). When considering more restrictive regulations, such as the US Environmental Protection Agency ($<235 \text{ MPN}/100 \text{ mL}$), just 15% of the samples presented conditions for primary contact recreation. The fecal coliform observations support the assertion that sewage is released in the watersheds without adequate or any treatment, a common practice in the coastal systems of South Brazil (Cabral et al., 2019; Garbossa et al., 2017; Netto et al., 2018).

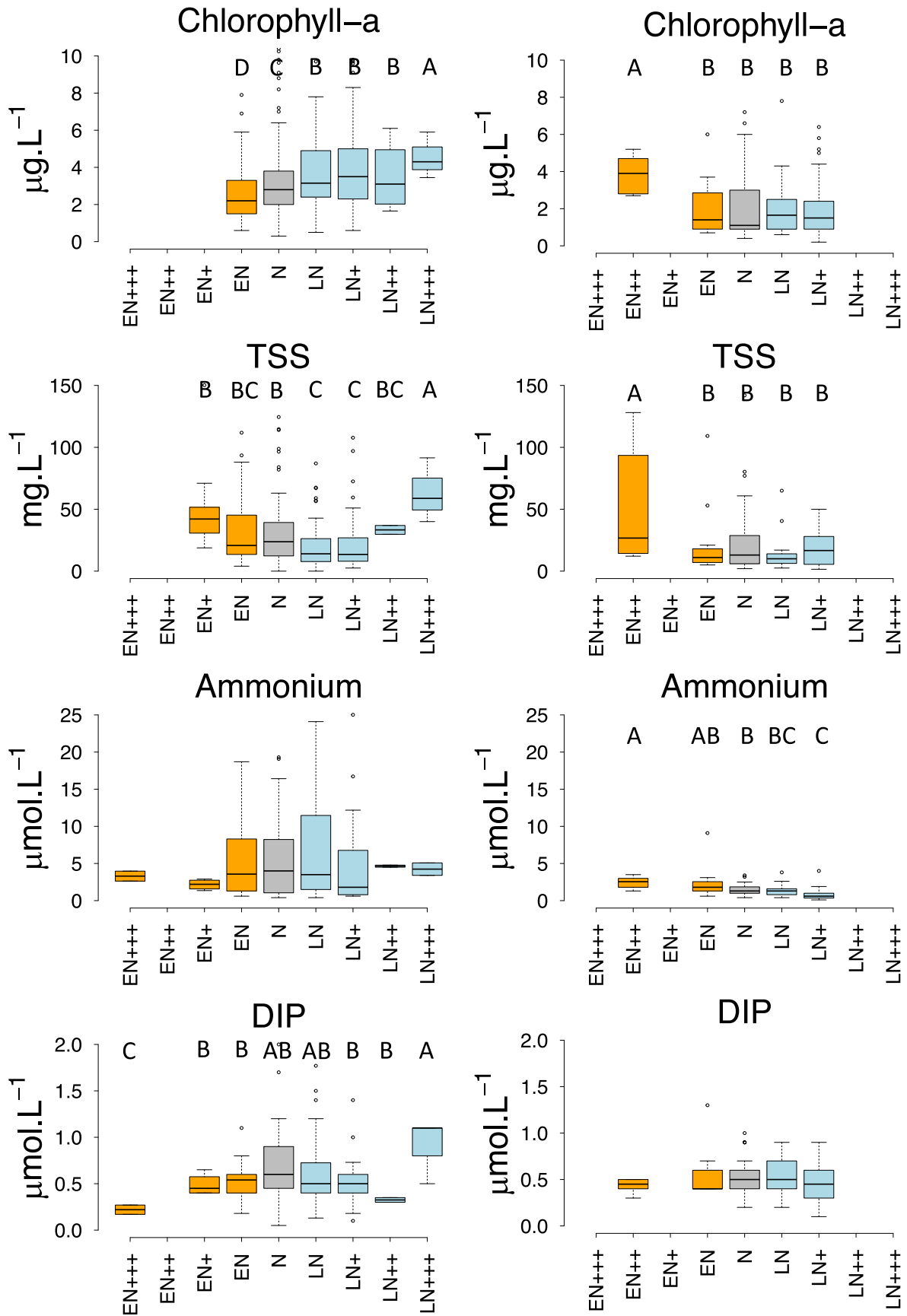
4.2. Seasonal variability across the watershed-bay-shelf continuum

Meteorological events and the water masses seasonality had strong control over the biogeochemistry and ecosystem metabolism of BSCI. In the summer, the synergetic effects of multiple eutrophic rivers' outflow, enhanced by the rainfall and sewage discharges, concomitantly with SACW upwelling boosted the biogeochemical processes and an autotrophic metabolism inside the bays. Oceanic P inputs occurred mainly to the South Bay in the summer and fall, while N inputs predominated in the North Bay during summer and spring. Interestingly, since these nutrients limit phytoplankton production in each bay, respectively, they favored autotrophy and new primary production. Maximum concentrations of chlorophyll-a were also found in the summer, similar to other systems in Brazil (Abreu et al., 2010; Barrera-Alba et al., 2019). In the rivers, however, primary productivity seems to be limited by turbidity. Pan et al. (2016) established a maximum threshold of 12 NTU for phytoplankton growth since chlorophyll-a was close to zero above those values. Turbidity equal or above 12 NTU was found in 76% of the

Fig. 9. Boxplot (minimum, maximum, median, first quartile, third quartile, and outliers) of the chlorophyll-a, TSS, ammonium and DIP in the bays and continental shelf across ENSO events. When significant ($p < 0.05$), upper-case letters indicate the Kruskal-Wallis pairwise comparison test results, where $A > B > C > D$. Legend information in the Fig. 8.

North and South Bays

Continental Shelf



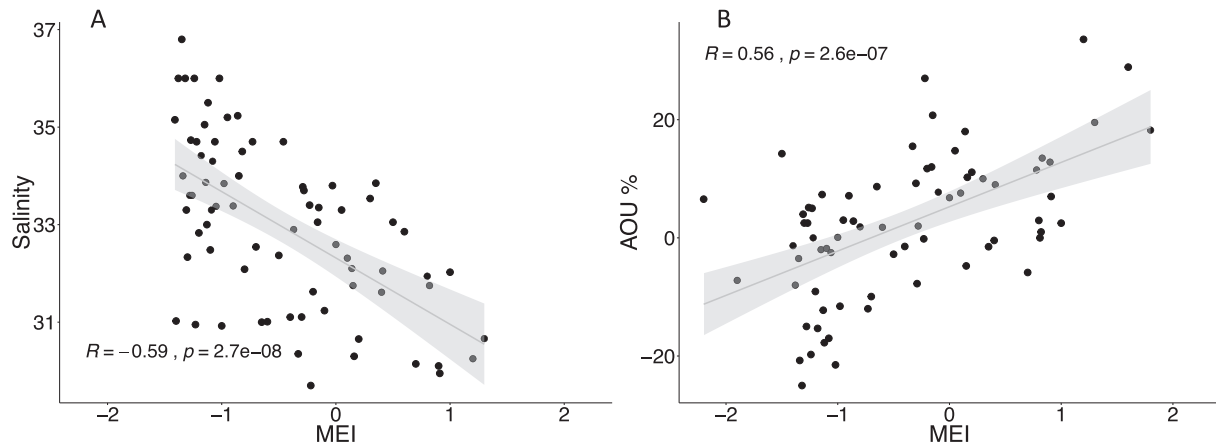


Fig. 10. Scatter plot between a) salinity and b) AOU (apparent oxygen utilization) and the multivariate ENSO index, considering MEI mean values, both in the bays and continental shelf. Pearson correlation algorithm was used to obtain the p and R values. Positive (>0.5) and negatives (<-0.5) MEI values indicate El Niño and La Niña events, respectively.

samples in the rivers during summer, suggesting that phytoplankton might be inhibited, as observed in other systems (Cloern, 1999; Tasic et al., 2019; Xu et al., 2013). In the fall, when precipitation decreases, the relative stability of the water column and still high concentration of nutrients allowed phytoplankton growth. High chlorophyll- a ($>10 \mu\text{g.L}^{-1}$) and hypoxia were observed in 39% and 33% of the samples in the rivers during fall, respectively, the highest frequencies among all seasons.

Denitrification predominates in both bays during summer, removing N out of the water column and limiting primary production, especially in the North Bay. Denitrification also increases over the SC continental shelf during summer, associated with organic matter mineralization in the oxygen-depleted SACW (Bordin et al., 2019). In the bays, sediment characteristics might be influencing denitrification, since the North Bay is composed by mud enriched with organic matter and nitrogen, whereas the bottom of South Bay is mostly formed by sand (Bonetti et al., 2007). Although denitrification was estimated by the LOICZ

model, our results oscillated between zero and $-2 \text{ mmolN.m}^{-2}.\text{day}^{-1}$, consistent with the values found in 20 other estuaries and coastal lagoons around the world, where denitrification was measured by membrane inlet mass spectrometry (Cornwell et al., 2014). N fixation contributed with 13% of total DIN, suggesting little contribution of diazotrophs, however, *Trichodesmium* colonies, including toxic species, have been reported close to the BSCI and in the continental shelf, indicating potential autochthonous N inputs (Proença et al., 2009; Röhrig et al., 2018).

In the winter, the metabolism shifted to heterotrophic and regeneration of organic matter predominates in the bays, concomitantly with high residence time, pheophytin- a and trophic state (TRIX). The metabolism of estuarine systems appear to be regulated by the exchange time, where heterotrophic conditions are directly correlated with high water residence time (Bricker et al., 2008; Swaney et al., 2011). Cold fronts associated to southerly winds in the winter transports oceanic waters to the shore by Ekman pumping, favoring water retention and organic

Table 4

Level of susceptibility to eutrophication by the pressure (IF), state (EuC) and response (FO) components and the overall classification grade by the ASSETS model for the North and South Bays by decade. The future outlooks for the next decade (2020's) were estimated considering the follow scenarios: 1 - (population increasing by 25% and same effluent treatment on 27% of urban population), 2 - (population increasing by 25% and 100% of effluent treatment) and 3 - (same population (~1.1 million) and 100% of effluent treatment). TRIX and LOICZ decadal trophic classification were also included, following Giovanardi and Vollenweider (2004) for TRIX and Nixon (1995) for the organic carbon production, here estimated by the LOICZ model (NEM, $\text{gC.m}^{-2}.\text{year}^{-1}$).

System	North bay			South bay		
	1990's	2000's	2010's	1990's	2000's	2010's
Decade						
Influencing factors (IF)	Moderate high	Moderate high	Moderate high	High	High	High
Eutrophic conditions (EuC)	Moderate high	Moderate high	Moderate high	Moderate high	Moderate high	High
Future outlook (FO1)	-	-	No change	-	-	No change
Future outlook (FO2)	-	-	No change	-	-	No change
Future outlook (FO3)	-	-	No change	-	-	No change
ASSETS overall score	Poor	Poor	Poor	Bad	Bad	Bad
TRIX (index)	-	Bad eutrophic (6.1)	Bad eutrophic (6.1)	-	Poor mesotrophic (5.8)	Bad eutrophic (6.2)
LOICZ (NEM)	-	Good oligotrophic (53)	Poor mesotrophic (129)	Very bad hypereutrophic (695)	Poor mesotrophic (133)	Bad eutrophic (376)

matter (OM) mineralization in the coastal systems of south Brazil (Abreu et al., 2010; Cabral and Fonseca, 2019; Möller et al., 2008). The same variation in the metabolism was described in the continental shelf, where new production was enhanced in the summer, associated to the SACW upwelling up to the 20 m isobath, and OM regeneration in the winter, related to the PPW (Bordin et al., 2019; Brandini et al., 2014). Moreover, bacterioplankton abundance and biomass in the shelf was reported to be 10 times higher in the winter than summer, mostly concentrated in the areas under the influence of the PPW (Fontes et al., 2018), fueling net heterotrophy and corroborating our results. Although the main nutrient pool of PPW is assimilated in higher latitudes ($>30^{\circ}\text{S}$), the residual DIP and silicate, combined with OM remineralization, can stimulate primary productivity and algal blooms during winter (Brandini et al., 2014).

The effects of oceanic water intrusion during winter were detected up the estuarine zone of the rivers, associated with low rainfall, as observed in other subtropical systems (Netto et al., 2018). Salinity levels were three times higher in the winter than other seasons, improving the rivers water quality due to the decrease of continental runoff and the improvement of mixing processes with marine waters. The winter-time was also the only season where most of DO and fecal coliform were in compliance with regulation thresholds. DIN also decreased in winter, but DIP did not change among seasons, probably due to the strong control over P fluxes by the sediment, as previously reported for the estuaries of BSCI (Pagliosa et al., 2005). Overall, the estuarine zone of the rivers showed a clear pattern, where the worst-case scenarios were found in the summer and fall due to high wastewater runoff, precipitation rates and population fluctuation pressure. Eutrophic conditions were sustained until late fall, when the intrusion of oceanic waters gained strength, boosting water renew. However, the low oxygen levels and high pheophytin indicated that the estuarine zone of the rivers are potentially heterotrophic most of the time, acting as a source of nutrients to the BSCI. The LOICZ model showed that nutrient inputs from the rivers are metabolized inside the bays, except during winter, when heterotrophic conditions shift the system from sink to source of nutrients. A conceptual model about the interactions among the meteorological patterns, water masses seasonality and the biogeochemical processes in watershed-bay-shelf continuum is showed in the Fig. 11.

4.3. ENSO effects in the biogeochemistry

The El Niño Southern Oscillation (ENSO) plays an important role in the meteorological patterns of South America, and it also shifts the physical and biogeochemical characteristics of the estuarine systems of South Brazil (Abreu et al., 2010; Netto et al., 2018). There were nine El Niño and eight La Niña events between 1993 and 2019, persisting from weeks to years and showing different levels of intensity. Extreme rainfall in the southeastern sector of South America is expected during El Niño, whereas abnormally droughts usually occurs during La Niña (Grimm and Tedeschi, 2009). Considering all the main rivers that drain to the BSCI and all the dataset used in this study, mean freshwater runoff into the North and South bay were about 12 and 20 $\text{m}^3 \cdot \text{s}^{-1}$, respectively. However, we found that during extreme rainfall ($>250 \text{ mm} \cdot \text{month}^{-1}$), observed in 13% of the months between 1993 and 2019, freshwater runoff can increase up to 114 $\text{m}^3 \cdot \text{s}^{-1}$ in the North bay and 273 $\text{m}^3 \cdot \text{s}^{-1}$ in the South bay, approximately ten times more than normal conditions.

One of the effects of high runoff in estuarine systems is an abrupt drop of residence time and chlorophyll-a, such as observed in the San Francisco Bay when outflows exceed 200–300 $\text{m}^3 \cdot \text{s}^{-1}$ (Cloern, 2019) and other coastal systems around the world (Abreu et al., 2010; Barrera-Alba et al., 2019; Chen et al., 2018; Odebrecht et al., 2015; Sathicq et al., 2015). The same pattern might be occurring in the BSCI; low chlorophyll-a and nutrients were measured during El Niño, especially in the 1997–1998 event, one of strongest ever recorded (Wolter and Timlin, 2011). Moreover, the GAM indicated that the ENSO and

salinity have strong controls on chlorophyll-a variability inside the bay, supporting our hypothesis. In the continental shelf, high concentrations of chlorophyll-a and ammonium were measured during El Niño, increasing the trophic state and potentially impacting the primary productivity, such as observed in the Gulf of Farallones (USA) during the 1997–1998 El Niño (Wilkerson et al., 2002).

The influence of the South Bay's plume over the continental shelf can reach up to 100 m isobath, such as measured in a transect perpendicular to the coast in the fall of 2019 (Fig. 6), which was under a weak El Niño event. The plume of the North Bay, as well as of other eutrophic coastal systems in the region (e.g. Itajaí river, Tijucas river, Camboriú river, and Babitonga Bay) have been reported to modify the plankton food web structure over the continental shelf, also driving harmful algal blooms (HABs), but little is known about the coupled effects of ENSO in these processes (Becker et al., 2018; Menezes et al., 2019; Rörig et al., 2018). The combined effect of estuarine waters with the intrusion of nutrient-rich water masses, such as the PPW, have also been described as a major mechanism driving dinoflagellate (e.g. *Dinophysis acuminata*) blooms in the BSCI and other coastal ecosystems of South Brazil (Alves et al., 2018). These organisms produce okadaic acid and dinophysistoxins, which causes diarrhetic shellfish poisoning, the main reason for mollusk aquaculture and extraction bans in the region, since these toxins accumulate in mussels, oysters and fishes (Alves et al., 2018).

The PPW transport different phytoplankton species, especially during El Niño events, since extreme rainfall strengthens the overflow of the Plata river watershed (~ 3 million km^2), the second largest in South America (Machado et al., 2013; Sathicq et al., 2015). The longest (~ 55 days) HAB reported in Brazil occurred in Santa Catarina during the fall-winter of 2016, associated with a strong PPW intrusion and the 2015–2016 El Niño, when economic losses of shellfish aquaculture were up to 4 million US dollars (Proença et al., 2017). The major estuarine systems of Santa Catarina have elevated trophic conditions, favoring episodic blooms of opportunistic phytoplankton species, such as *Dinophysis* spp. and *Pseudo-nitzschia* spp., the latter of which produces domoic acid, related to amnesic shellfish poisoning (Alves et al., 2018; Rörig et al., 2018). While dinoflagellate blooms are found in the winter, diatom blooms usually occur in the late-spring and late-summer in south Brazil, causing the embargo of shellfish aquaculture for a period of weeks to months (Fernandes et al., 2013). Although there is less water runoff during La Niña, continuous sewage discharge fertilizes the bay with nutrients. The highest levels of chlorophyll-a inside the bays were found during very strong La Niña, as also observed in Babitonga bay and Patos lagoon, associated with high water residence time and anthropogenic nutrient sources (Alves et al., 2018; Odebrecht et al., 2015).

4.4. Long-term trends and eutrophication management approaches

Although the water quality parameters in estuarine systems fluctuate across multiple time scales (Cloern, 2019), some trends were observed in the BSCI, such as the shift of the NP ratio from P to N limiting and the increase of suspended solids (TSS) in the most recent years. Silicate, on the other hand, seems to be decreasing, indicating that the TSS might be composed of organic materials from sewage, correlating with DIP increase. HABs have become more frequent over the coast of Santa Catarina in the last years and, although the actual cause is not clear yet, it was suggested that aquaculture and sewage runoff might be contributing to this trend, especially for *Pseudo-nitzschia* spp. blooms (Rörig et al., 2018). The GAM suggested that chlorophyll-a has increased through the years, associated with high temperatures. The frequency of extreme events, such as heat waves and intense rainfall, have also increased in the region, favoring HABs (Gouvêa et al., 2017; Nunes and Silva, 2013).

The future scenarios of the ASSETS model indicated that the BSCI has been showing susceptibility to eutrophication since the 1990's and that

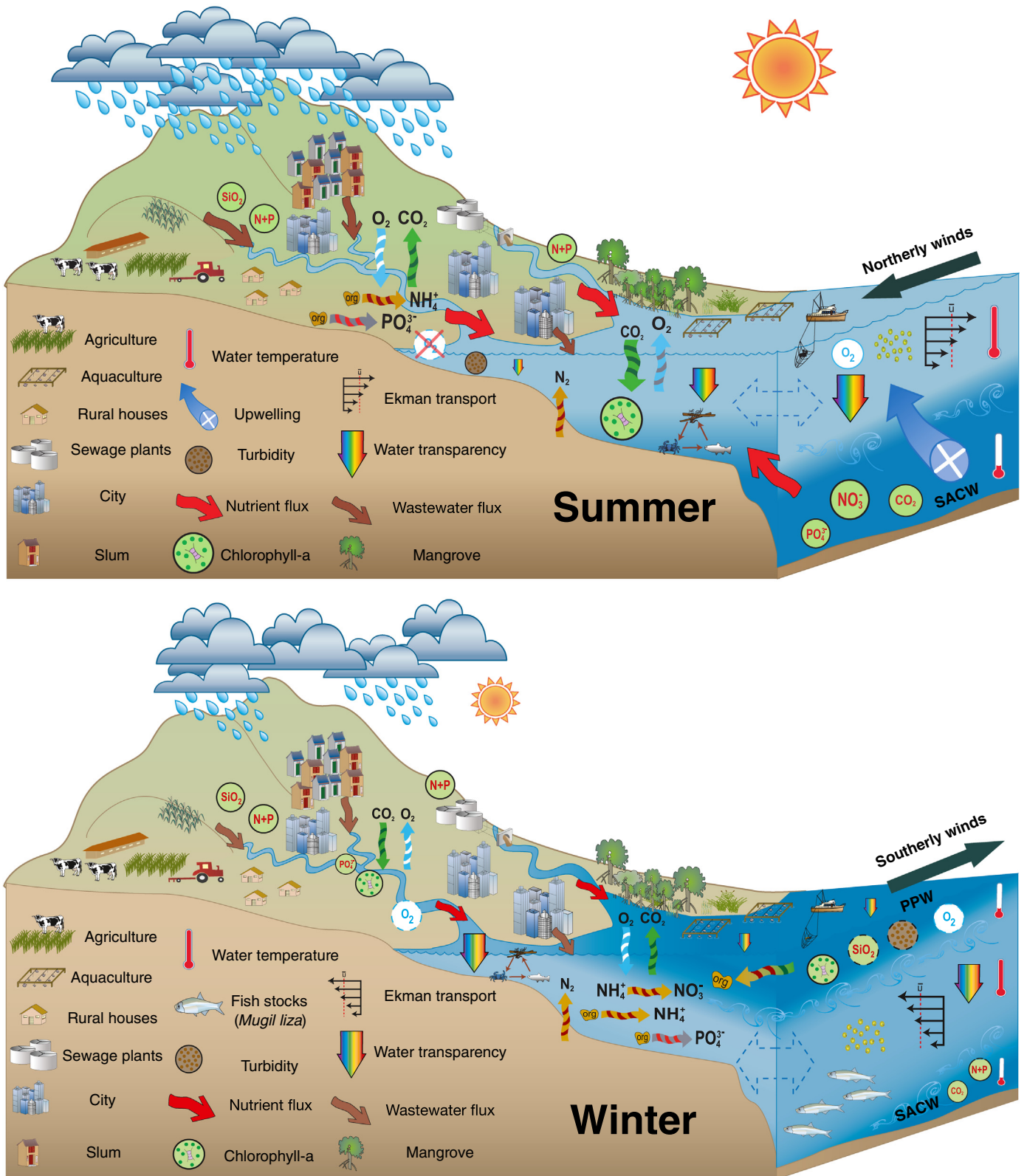


Fig. 11. Conceptual model of the physical and biogeochemical seasonality in the watershed-bay-shelf continuum. Symbols and images are courtesy of the Integration and Application Network, University of Maryland Center for Environmental Science (<https://ian.umces.edu>).

this condition will likely remain the same in the next decade as a result of high nutrient loads and periodic HABs. It is worth mentioning that even considering 100% of effluent treatment, the bays remained susceptible to eutrophication given the moderate flushing time (~40 days) and

seasonal influence of nutrient-rich oceanic water masses. Furthermore, the reduction of anthropogenic nutrient loads alone might not be able to quickly revert eutrophication, since other mechanisms, such as sediment nutrient release and environmental characteristics, may sustain

eutrophic conditions for years or even decades (Duarte et al., 2009; Smith and Schindler, 2009).

While our dataset starts in 1993, previous studies using sediment cores traced carbon and nutrient levels in the BSCI back to 1880 through isotope techniques (Lamego et al., 2017). They found that total carbon, nitrogen and phosphorus increased towards the most recent years, concomitantly with population and urbanization growth, showing a gradual evolution of eutrophication. The $\delta^{15}\text{N}$ shifted to more enriched values since the 1990's in the North Bay, while the $\delta^{13}\text{C}$ indicated that the main source of organic matter is the phytoplankton. Denitrification is an important mechanism to regulate eutrophication (Abreu et al., 2006), which removes the lighter ^{14}N faster than the ^{15}N isotope, might explaining the $\delta^{15}\text{N}$ increase found by Lamego et al. (2017). As the LOICZ model showed, about 60% of DIN is removed by denitrification in the North Bay, similar to the rates found in coastal systems of New Zealand (Zeldis and Swaney, 2018).

The lack of an effective sewage collection and treatment in the BSCI watersheds threatens its biodiversity and ecosystems services. For example, we found N as ammonia up to $549 \mu\text{gNH}_3\text{-N.L}^{-1}$ in the rivers, well above the recommendation for waters of high conservation value ($160 \mu\text{gNH}_3\text{-N.L}^{-1}$), but near $460 \mu\text{gNH}_3\text{-N.L}^{-1}$, considered as moderately disturbed (Batley and Simpson, 2009). Although ammonia is probably related to sewage, other studies have found high concentrations of copper in the BSCI, up to 213nmol.L^{-1} , associated with anti-fouling paints and industrial activities (Mello et al., 2005). The toxicity effects of these compounds are still unknown, however, they are worrying, since the BSCI is a nursery ground for several fish stocks and endangered species (Cattani et al., 2018; Rossi-Santos and Flores, 2009; Wedekin et al., 2007). Also, as demonstrated by this and other studies (Paquette et al., 2016), organic enriched waters from the bays can reach the shelf, including marine protected areas (e.g. Arvoredo archipelago), threatening the sensitive species established there, such as the southernmost coral-line algal bank of the western south Atlantic.

In order to better manage the eutrophication problem in the BSCI, multiple approaches at ecosystem-scale are needed. First, the sewage pipelines must be expanded to all watersheds, as well as the treatment plants, making sure that even the most susceptible communities in the region will have access to basic sanitation. The WWTPs must also have tertiary treatment (nutrient removal) since they discharge into the bay, which is unable to process the current loads due its moderate flushing time. Other strategies include enhance carbon and nutrient sequestration by protecting and recovering wetlands, such as the seagrass meadows, salt marches and mangroves around the bays. The remaining mangrove patches of BSCI have been deforested in the last decades, compromising its services and functions (Pagliosa et al., 2006). For example, mass mortality (~95% of the population died) of an important mussel (*Anomalocardia brasiliana*) for traditional communities in one of these mangroves was related to eutrophication and heat waves (Carneiro et al., 2020). The synergetic effects of local and global stressors might compromise the biodiversity, water quality and food security of BSCI if mitigation strategies and environmental monitoring were not taken into account in the public policies.

5. Conclusions

The BSCI watersheds are under high anthropic pressure, where the most urbanized systems are more susceptible to eutrophication due to wastewater runoff. Worst-case scenarios in the rivers were found in the summer and fall, associated with sewage inputs boosted by rainfall and mass tourism. In the bays, the eutrophication assessment methods resulted in similar feedbacks, indicating that trophic status oscillated from moderate to high over the last three decades. The seasonal effect of oceanic water masses (SACW and PPW) and rainfall events drive the ecosystem metabolism and the water residence time of the bays, from new primary production in the summer to regeneration of organic matter in the winter, coupled with low and high residence time,

respectively. Large-scale events, such as El Niño, have strong controls over the transport of materials in the watershed-bay-shelf continuum. The overall synergetic effects of continental runoff associated with meso-scale phenomena (e.g. oceanic water masses) have important implications for the occurrence of algal blooms in south Brazil, both during summer and winter. Effective actions to mitigate eutrophication include addressing nutrient sources, upgrading the WWTPs coverage and technology, wetlands restoration and long-term monitoring. In this way, the anthropic pressures might decrease, also providing better water quality to sustain the biodiversity and ecosystem services of BSCI.

CRÉDIT authorship contribution statement

AC and AF designed the research. AF, LG, JPF and KB provided data and comments. AC interpreted the data and wrote the paper with recommendations provided by AF and CB.

Declaration of competing interest

The authors declare that they have no known competing financial interests or personal relationships that could have appeared to influence the work reported in this paper.

Acknowledgments

We would like to thank all the researches and students who collaborate to produce the data used in this article. This study was financed in part by the Coordenação de Aperfeiçoamento de Pessoal de Nível Superior - Brasil (CAPES) and the Fundação de Amparo à Pesquisa e Inovação do Estado de Santa Catarina - Brasil (FAPESC) - Finance Code Edital 3/2017.

Appendix A. Supplementary data

Supplementary data to this article can be found online at <https://doi.org/10.1016/j.scitotenv.2020.141553>.

References

- Abreu, P.C., Costa, C.S.B., Bemvenuti, C., Odebrecht, C., Graneli, W., Anesio, A.M., 2006. Eutrophication processes and trophic interactions in a shallow estuary: preliminary results based on stable isotope analysis ($\delta^{13}\text{C}$ and $\delta^{15}\text{N}$). *Estuar. Coasts* 29, 277–285. <https://doi.org/10.1007/BF02781996>.
- Abreu, P.C., Bergesch, M., Proença, L.A., Garcia, C.A.E., Odebrecht, C., 2010. Short- and long-term chlorophyll a variability in the shallow microtidal Patos Lagoon Estuary, Southern Brazil. *Estuar. Coasts* 33, 554–569. <https://doi.org/10.1007/s12237-009-9181-9>.
- Alves, T.P., Schramm, M.A., Tamanaha, M. da S., Proença, L.A. de O., 2010. Implementação e avaliação do monitoramento de algas nocivas e de fitotoxinas em um cultivo de moluscos em Florianópolis - SC. *Atlântica* 32, 71–77. <https://doi.org/10.5088/atl.2010.32.1.71>.
- Alves, T.P., Schramm, M.A., Proença, L.A.O., Pinto, T.O., Mafra, L.L., 2018. Interannual variability in *Dinophysis* spp. abundance and toxin accumulation in farmed mussels (*Perna perna*) in a subtropical estuary. *Environ. Monit. Assess.* 190. <https://doi.org/10.1007/s10661-018-6699-y>.
- ANA, 2017. Agência Nacional de Águas (Brasil). Atlas esgotos: despoluição de bacias hidrográficas. Secretaria Nacional de Saneamento Ambiental <http://atlas.esgotos.ana.gov.br/>.
- Anderson, M.J., 2017. Permutational multivariate analysis of variance (PERMANOVA). Wiley StatsRef: Statistics Reference Online. John Wiley & Sons, Ltd, Chichester, UK, pp. 1–15. <https://doi.org/10.1002/9781118445112.stat07841>.
- Barletta, M., Lima, A.R.A., Costa, M.F., 2019. Distribution, sources and consequences of nutrients, persistent organic pollutants, metals and microplastics in South American estuaries. *Sci. Total Environ.* 651, 1199–1218. <https://doi.org/10.1016/j.scitotenv.2018.09.276>.
- Barrera-Alba, J.J., Cesar, P., Rivera, D., 2019. Seasonal and inter-annual variability in phytoplankton over a 22-year period in a tropical coastal region in the southwestern Atlantic Ocean. *Cont. Shelf Res.* 176, 51–63. <https://doi.org/10.1016/j.csr.2019.02.011>.
- Batley, G.E., Simpson, S.L., 2009. Development of guidelines for ammonia in estuarine and marine water systems. *Mar. Pollut. Bull.* 58, 1472–1476. <https://doi.org/10.1016/j.marpolbul.2009.06.005>.
- Becker, É.C., Eiras Garcia, C.A., Freire, A.S., 2018. Mesozooplankton distribution, especially copepods, according to water masses dynamics in the upper layer of the Southwestern Atlantic shelf (26°S to 29°S). *Cont. Shelf Res.* 166, 10–21. <https://doi.org/10.1016/j.csr.2018.06.011>.

- Bell, T.G., Johnson, M.T., Jickells, T.D., Liss, P.S., 2007. Ammonia/ammonium dissociation coefficient in seawater: a significant numerical correction. *Environ. Chem.* 4, 183. <https://doi.org/10.1071/EN07032>.
- Benson, B.B., Krause, D., 1984. *The Concentration and Isotopic Fractionation of Oxygen Dissolved in Freshwater and Seawater in Equilibrium With the Atmosphere*. vol. 29 pp. 620–632.
- Bonetti, C., Bonetti, J., Barcellos, R.L., 2007. Caracterização sedimentar e geoquímica de sistemas costeiros com ênfase na avaliação da influência de sítios de cultivo de moluscos. *Sistemas de Cultivos Aquícolas Na Zona Costeira Do Brasil: Recursos, Tecnologias, Aspectos Ambientais e Sócio - Econômicos*, pp. 139–149.
- Bordin, L., Machado, C., Carvalho, M., Freire, A.S., Fonseca, A.L.D.O., 2019. Nutrient and carbon dynamics under the water mass seasonality on the continental shelf at the South Brazil Bight. *J. Mar. Syst.* 189, 22–35. <https://doi.org/10.1016/j.jmarsys.2018.09.006>.
- Brandini, F., Nogueira, M., Simião, M., Carlos Ugaz Codina, J., Almeida Noernberg, M., 2014. Deep chlorophyll maximum and plankton community response to oceanic bottom intrusions on the continental shelf in the South Brazilian Bight. *Cont. Shelf Res.* 89, 61–75. <https://doi.org/10.1016/j.csr.2013.08.002>.
- Brandini, F.P., Tura, P.M., Santos, P.P.G.M., 2018. Ecosystem responses to biogeochemical fronts in the South Brazil Bight. *Prog. Oceanogr.* 164, 52–62. <https://doi.org/10.1016/j.pocean.2018.04.012>.
- Breitburg, D., Levin, L.A., Oschlies, A., Grégoire, M., Chavez, F.P., Conley, D.J., Garçon, V., Gilbert, D., Gutiérrez, D., Isensee, K., Jacinto, G.S., Limburg, K.E., Montes, I., Naqvi, S.W.A., Pitcher, G.C., Rabalais, N.N., Roman, M.R., Rose, K.A., Seibel, B.A., Telszewski, M., Yasuhara, M., Zhang, J., 2018. Declining oxygen in the global ocean and coastal waters. *Science* (80-), 359 <https://doi.org/10.1126/science.aam7240>.
- Bricker, S.B., Ferreira, J.G., Simas, T., 2003. An integrated methodology for assessment of estuarine trophic status. *Ecol. Model.* 169, 39–60. [https://doi.org/10.1016/S0304-3800\(03\)00199-6](https://doi.org/10.1016/S0304-3800(03)00199-6).
- Bricker, S.B., Longstaff, B., Dennison, W., Jones, A., Boicourt, K., Wicks, C., Woerner, J., 2008. Effects of nutrient enrichment in the nation's estuaries: a decade of change. *Harmful Algae* 8, 21–32. <https://doi.org/10.1016/j.hal.2008.08.028>.
- Brugnoli, E., Muniz, P., Venturini, N., Brena, B., Rodríguez, A., 2019. Assessing multimetric trophic state variability during an ENSO event in a large estuary (Rio de la Plata, South America). *Reg. Stud. Mar. Sci.*, 100565 <https://doi.org/10.1016/j.rsma.2019.100565>.
- Cabral, A., Fonseca, A., 2019. Coupled effects of anthropogenic nutrient sources and meteorological events in the trophic state of a subtropical estuarine system. *Estuar. Coast. Shelf Sci.* 225, 106228. <https://doi.org/10.1016/j.ecss.2019.05.010>.
- Cabral, A., Bercovich, M.V., Fonseca, A., 2019. Implications of poor-regulated wastewater treatment systems in the water quality and nutrient fluxes of a subtropical coastal lagoon. *Reg. Stud. Mar. Sci.*, 29 <https://doi.org/10.1016/j.rsma.2019.100672>.
- Carneiro, A.P., Soares, C.H.L., Manso, P.R.J., Pagliosa, P.R., 2020. Impact of marine heat waves and cold spell events on the bivalve *Anomalocardia flexuosa*: a seasonal comparison. *Mar. Environ. Res.* 156, 104898. <https://doi.org/10.1016/j.marenvres.2020.104898>.
- Cattani, A.P., Cardoso, O.R., Ribeiro, G.C., Soeth, M., Silva, M.H., Clezar, L., Pichler, H.A., Spach, H.L., 2018. Fish species richness in shallow environments of the Island of Santa Catarina, Southern Brazil. *Rev. CEPSUL - Biodiversidade e Conserv. Mar.* 7, 1–16.
- Chen, N., Krom, M.D., Wu, Y., Yu, D., Hong, H., 2018. Storm induced estuarine turbidity maxima and controls on nutrient fluxes across river-estuary-coast continuum. *Sci. Total Environ.* 628–629, 1108–1120. <https://doi.org/10.1016/j.scitotenv.2018.02.060>.
- Clarke, K.R., Warwick, R.M., 2001. *Change in Marine Communities: An Approach to Statistical Analysis and Interpretation*. 2nd edition. Prim. Plymouth UK (doi:1).
- Cloern, J.E., 1999. The relative importance of light and nutrient limitation of phytoplankton growth: a simple index of coastal ecosystem sensitivity to nutrient enrichment. *Aquat. Ecol.* 33, 3–16.
- Cloern, J.E., 2019. Patterns, pace, and processes of water-quality variability in a long-studied estuary. *Limnol. Oceanogr.* 64, S192–S208. <https://doi.org/10.1002/lno.10958>.
- Cloern, J.E., Jassby, A.D., 2010. Patterns and Scales of Phytoplankton Variability in Estuarine – Coastal Ecosystems. , pp. 230–241 <https://doi.org/10.1007/s12237-009-9195-3>.
- Cloern, J.E., Abreu, P.C., Carstensen, J., Chauvaud, L., Elmgren, R., Grall, J., Greening, H., Johansson, J.O.R., Kahru, M., Sherwood, E.T., Xu, J., Yin, K., 2016. Human activities and climate variability drive fast-paced change across the world's estuarine-coastal ecosystems. *Glob. Chang. Biol.* 22, 513–529. <https://doi.org/10.1111/gcb.13059>.
- Cloern, J.E., Jassby, A.D., Schraga, T.S., Nejad, E., Martin, C., 2017. Ecosystem variability along the estuarine salinity gradient: examples from long-term study of San Francisco Bay. *Limnol. Oceanogr.* 62, S272–S291. <https://doi.org/10.1002/lno.10537>.
- Cornwell, J.C., Glibert, P.M., Owens, M.S., 2014. Nutrient fluxes from sediments in the San Francisco Bay Delta. *Estuar. Coasts* 37, 1120–1133. <https://doi.org/10.1007/s12237-013-9755-4>.
- Dan, S.F., Liu, S.M., Udoh, E.C., Ding, S., 2019. Nutrient biogeochemistry in the Cross River estuary system and adjacent Gulf of Guinea, South East Nigeria (West Africa). *Cont. Shelf Res.* 179, 1–17. <https://doi.org/10.1016/j.csr.2019.04.001>.
- Duarte, C.M., Conley, D.J., Carstensen, J., Sánchez-Camacho, M., 2009. Return to Neverland: shifting baselines affect eutrophication restoration targets. *Estuar. Coasts* 32, 29–36. <https://doi.org/10.1007/s12237-008-9111-2>.
- Dupra, V., Smith, S.V., Marshall Crossland, J.L., Crossland, C.J., 2000. Estuarine systems of the South China Sea region: carbon, nitrogen and phosphorus fluxes. *LOICZ Reports & Studies No. 14* <https://doi.org/10.13140/RG.2.1.4708.5283>.
- Fernandes, L.F., Cavalcante, K.P., Luis, L.A., Schramm, M.A., 2013. Blooms of *Pseudo-nitzschia pseudodelicatissima* and *P. calliantha*, and associated domoic acid accumulation in shellfish from the South Brazilian coast. *Diatom Res* 28, 381–393. <https://doi.org/10.1080/0269249X.2013.821424>.
- Ferreira, J.G., Bricker, S.B., Simas, T.C., 2007. Application and sensitivity testing of a eutrophication assessment method on coastal systems in the United States and European Union. *J. Environ. Manag.* 82, 433–445. <https://doi.org/10.1016/j.jenvman.2006.01.003>.
- Fontes, M.L.S., Berri, A., Carvalho, M., Fonseca, A.L.O., Antônio, R.V., Freire, A.S., 2018. Bacterioplankton abundance and biomass stimulated by water masses intrusions from the Southern Brazilian Shelf (between 25°57'S and 29°24'S). *Cont. Shelf Res.* 164, 28–36. <https://doi.org/10.1016/j.csr.2018.05.003>.
- Garbosa, L.H.P., Vanz, A., Fernandes, L., Souza, R.V. de, Vianna, L.F., Rupp, G., 2014. Modeling and validation of the Santa Catarina Island bays hydrodynamics based on astronomical tides and measured tides. 11th Int. Conf. Hydroinformatics, p. 8 <https://doi.org/10.13140/2.1.5123.6163>.
- Garbosa, L.H.P., Souza, R.V., Campos, C.J.A., Vanz, A., Vianna, L.F.N., Rupp, G.S., 2017. Thermotolerant coliform loadings to coastal areas of Santa Catarina (Brazil) evidence the effect of growing urbanisation and insufficient provision of sewerage infrastructure. *Environ. Monit. Assess.* 189, 27. <https://doi.org/10.1007/s10661-016-5742-0>.
- Giovanardi, F., Vollenweider, R.A., 2004. *Trophic Conditions of Marine Coastal Waters: Experience in Applying the Trophic Index TRIX to Two Areas of the Adriatic and Tyrrhenian Seas*. vol. 63 pp. 199–218.
- Gordon, D.C., Boudreau, P.R., Mann, K.H., Ong, J.-E., Silvert, W.L., Smith, S.V., Wattayakorn, G., Wulff, F., Yanagi, T., 1996. *LOICZ Biogeochemical Modelling Guidelines*. <https://doi.org/10.13140/RG.2.1.5003.4401>.
- Gouvêa, L.P., Schubert, N., Martins, C.D.L., Sissini, M., Ramlov, F., Rodrigues, E.R. de O., Bastos, E.O., Freire, V.C., Maraschin, M., Carlos Simonassi, J., Varela, D.A., Franco, D., Cassano, V., Fonseca, A.L., Baruffi, J.B., Horta, P.A., 2017. Interactive effects of marine heatwaves and eutrophication on the ecophysiology of a widespread and ecologically important macroalgae. *Limnol. Oceanogr.* 62, 2056–2075. <https://doi.org/10.1002/lno.10551>.
- Grasshoff, K., Kremling, K., Ehrhardt, M., 1999. *Methods of Seawater Analysis, Methods of Seawater Analysis: Third, Completely Revised and Extended Edition*. Wiley <https://doi.org/10.1002/9783527613984>.
- Grimm, A.M., Tedeschi, R.G., 2009. ENSO and extreme rainfall events in South America. *J. Clim.* 22, 1589–1609. <https://doi.org/10.1175/2008JCLI2429.1>.
- Harding, L.W., Mallonee, M.E., Perry, E.S., Miller, W.D., Adolf, J.E., Gallegos, C.L., Paerl, H.W., 2019. Long-term trends, current status, and transitions of water quality in Chesapeake Bay. *Sci. Rep.* 9, 1–19. <https://doi.org/10.1038/s41598-019-43036-6>.
- Hoinaski, L., Franco, D., Haas, R., Martins, R.F., Lisboa, H.D.M., 2014. Investigation of rain-water contamination sources in the southern part of Brazil. *Environ. Technol. (United Kingdom)* 35, 868–881. <https://doi.org/10.1080/09593330.2013.854412>.
- Labasque, T., Chaumery, C., Aminot, A., Kergoat, G., 2004. *Spectrophotometric Winkler Determination of Dissolved Oxygen: Re-examination of Critical Factors and Reliability*. vol. 88 pp. 53–60.
- Lamego, F., da Silva, A.L.G., Simonassi, J.C., Nepomuceno, A., 2017. Reconstructing recent land-ocean changes in the Brazilian Southern Coast using sedimentary proxies and tracking airborne 210Pb. *J. Radioanal. Nucl. Chem.* 314, 2281–2299. <https://doi.org/10.1007/s10967-017-5623-1>.
- Le Moal, M., Gascuel-Oudou, C., Ménesguen, A., Souchon, Y., Étrillard, C., Levain, A., Moatar, F., Pannard, A., Souchu, P., Lefebvre, A., Pinay, G., 2019. Eutrophication: a new wine in an old bottle? *Sci. Total Environ.* 651, 1–11. <https://doi.org/10.1016/j.scitotenv.2018.09.139>.
- Li, R., Liu, S., Zhang, G., Ren, J., Zhang, J., 2012. Biogeochemistry of nutrients in an estuary affected by human activities: the Wanquan River estuary, eastern Hainan Island, China. *Cont. Shelf Res.*, 1–14 <https://doi.org/10.1016/j.csr.2012.02.013>.
- Machado, I., Barreiro, M., Calliari, D., 2013. Variability of chlorophyll-a in the Southwestern Atlantic from satellite images: seasonal cycle and ENSO influences. *Cont. Shelf Res.* 53, 102–109. <https://doi.org/10.1016/j.csr.2012.11.014>.
- Mello, L.C., Claudino, A., Rizzatti, I., Bortoluzzi, R.L., Zanette, D.R., 2005. Analysis of trace metals Cu²⁺, Pb²⁺ and Zn²⁺ in coastal marine water samples from Florianópolis, Santa Catarina State, Brazil. *J. Braz. Chem. Soc.* 16, 308–315. <https://doi.org/10.1590/S0103-50532005000300003>.
- Menezes, B.S., de Macedo-Soares, L.C.P., Freire, A.S., 2019. Changes in the plankton community according to oceanographic variability in a shallow subtropical shelf: SW Atlantic. *Hydrobiologia* 835, 165–178. <https://doi.org/10.1007/s10750-019-3936-5>.
- Mizerkowski, B.D., Hesse, K., Ladwig, N., Machado, C., Rosa, R., Araújo, T., Koch, D., 2012. Sources, Loads and Dispersion of Dissolved Inorganic Nutrients in Paranaguá Bay. , pp. 1409–1424 <https://doi.org/10.1007/s10236-012-0569-x>.
- Möller, O.O., Piola, A.R., Freitas, A.C., Campos, E.J.D., 2008. The effects of river discharge and seasonal winds on the shelf off southeastern South America. *Cont. Shelf Res.* 28, 1607–1624. <https://doi.org/10.1016/j.csr.2008.03.012>.
- Netto, S.A., Pagliosa, P.R., Colling, A., Fonseca, A.L., Brauko, K.M., 2018. Benthic estuarine assemblages from the Southern Brazilian Marine Ecoregion. In: Lana, P. da C., Bernardino, A.F. (Eds.), *Brazilian Estuaries, Brazilian Marine Biodiversity*. Springer International Publishing, Cham, pp. 177–212 https://doi.org/10.1007/978-3-319-77779-5_6.
- Nixon, S.W., 1995. *Coastal marine eutrophication: a definition, social causes, and future concerns*. *Ophelia* 41, 199–219.
- Nixon, S.W., 2009. Eutrophication and the microscope. *Hydrobiologia* 629, 5–19. <https://doi.org/10.1007/s10750-009-9759-z>.
- Nunes, A.B., Silva, G.C., 2013. Climatology of extreme rainfall events in eastern and Northern Santa Catarina State, Brazil: present and future climate. *Rev. Bras. Geofísica* 31, 413. <https://doi.org/10.22564/rbfg.v31i3.314>.
- Odebrecht, C., Abreu, P.C., Carstensen, J., 2015. Retention time generates short-term phytoplankton blooms in a shallow microtidal subtropical estuary. *Estuar. Coast. Shelf Sci.* 162, 35–44. <https://doi.org/10.1016/j.ecss.2015.03.004>.

- Ovalle, A.R.C., Silva, C.F., Rezende, C.E., Gatts, C.E.N., Suzuki, M.S., Figueiredo, R.O., 2013. Long-term trends in hydrochemistry in the Paraíba do Sul River, southeastern Brazil. *J. Hydrol.* 481, 191–203. <https://doi.org/10.1016/j.jhydrol.2012.12.036>.
- Pagliosa, P.R., Fonseca, A., Bosquilha, G.E., Braga, E.S., Barbosa, F.A.R., 2005. Phosphorus dynamics in water and sediments in urbanized and non-urbanized rivers in Southern Brazil. *Mar. Pollut. Bull.* 50, 965–974. <https://doi.org/10.1016/j.marpolbul.2005.04.005>.
- Pagliosa, P.R., Fonseca, A., Barbosa, F.A.R., Braga, E., 2006. Urbanization impact on subtropical estuaries: a comparative study of water properties in urban areas and in protected areas. *J. Coast. Res.* 731–735.
- Pan, C.W., Chuang, Y.L., Chou, L.S., Chen, M.H., Lin, H.J., 2016. Factors governing phytoplankton biomass and production in tropical estuaries of western Taiwan. *Cont. Shelf Res.* 118, 88–99. <https://doi.org/10.1016/j.csr.2016.02.015>.
- Paquette, M., Bonetti, C., Bitencourt, V., Bonetti, J., 2016. Spatial patterns of benthic foraminifera as a support to the oceanographic characterisation of Arvoredo biological marine reserve (South Atlantic, Brazil). *Mar. Environ. Res.* 114, 40–50. <https://doi.org/10.1016/j.marenvres.2015.12.012>.
- Pimenta, F.M., Kirwan, A.D., 2014. The response of large outflows to wind forcing. *Cont. Shelf Res.* 89, 24–37. <https://doi.org/10.1016/j.csr.2013.11.006>.
- Proença, L., Tamanaha, M., Fonseca, R., 2009. Screening the toxicity and toxin content of blooms of the cyanobacterium *Trichodesmium erythraeum* (Ehrenberg) in northeast Brazil. *J. Venom. Anim. Toxins Incl. Trop. Dis.* 15, 204–215. <https://doi.org/10.1590/S1678-91992009000200004>.
- Proença, L.A.O., Schramm, M.A., Alves, T.P., Piola, A.R., 2017. The extraordinary 2016 autumn DSP outbreak in Santa Catarina, Southern Brazil, explained by large-scale oceanographic processes. *Proceedings of the 17th International Conference on Harmful Algae. International Society for the Study of Harmful Algae 2017. International Society for the Study of Harmful Algae*, pp. 42–45.
- Rabalais, N.N., Diaz, R.J., Levin, L.A., Turner, R.E., Gilbert, D., Zhang, J., 2010. Dynamics and distribution of natural and human-caused hypoxia. *Biogeosciences* 7, 585–619. <https://doi.org/10.5194/bg-7-585-2010>.
- Rinaldi, A., Giovanardi, F., 2011. Contribution of Richard A. Vollenweider toward understanding eutrophication of the coastal adriatic sea. *Aquat. Ecosyst. Heal. Manag.* 14, 200–203. <https://doi.org/10.1080/14634988.2011.576990>.
- Rörig, L.R., da Silva Tamanaha, M., da Rosa Persich, G., França Schettini, C.A., Truccolo Schettini, E.C., 2018. Phytoplankton patterns and processes in a tropical-subtropical transition region: Santa Catarina Coast, Southern Brazil. *Plankton Ecology of the Southwestern Atlantic. Springer International Publishing, Cham*, pp. 269–288. https://doi.org/10.1007/978-3-319-77869-3_13.
- Rossi-Santos, M.R., Flores, P.A.C., 2009. Commensalism between guiana dolphins *Sotalia guianensis* and sea birds in the North Bay of Santa Catarina, Southern Brazil. *Open Mar. Biol. J.* 3, 77–82. <https://doi.org/10.2174/1874450800903010077>.
- Sathicq, M.B., Bauer, D.E., Gómez, N., 2015. Influence of El Niño Southern Oscillation phenomenon on coastal phytoplankton in a mixohaline ecosystem on the southeastern of South America: Río de la Plata estuary. *Mar. Pollut. Bull.* 98, 26–33. <https://doi.org/10.1016/j.marpolbul.2015.07.017>.
- Sewald, A.M., Raul, M., Rudorff, N.M., Bonetti, C., Luiz, L.A., 2012. Caracterização Química do Extrato Orgânico de Sedimentos em Áreas de Cultivo de Ostras e Mexilhões na Baía Sul de Florianópolis. *SC. Rev. Virtual Quim.* 4, 413–433. <https://doi.org/10.5935/1984-6835.20120032>.
- Silva, A.R. da, Fonseca, A.L.D.O., 2016. Eutrofização dos recursos hídricos como ferramenta para a compreensão das doenças de vinculação hídrica. *Geosul* 31, 247. <https://doi.org/10.5007/2177-5230.2016v31n62p247>.
- Silva, C., Ferreira, J.G., Bricker, S.B., DeValls, T.A., Martín-Díaz, M.L., Yáñez, E., 2011. Site selection for shellfish aquaculture by means of GIS and farm-scale models, with an emphasis on data-poor environments. *Aquaculture* 318, 444–457. <https://doi.org/10.1016/j.aquaculture.2011.05.033>.
- Silva, A.R. da, Fonseca, A.L.D.O., Rodrigues, C.J., Beltrame, Â. da V., 2016. Application of ecological indicators in coastal watershed under high pressure during summer period. *RBRH* 21, 537–548. <https://doi.org/10.1590/2318-0331.011615106>.
- Silveira, Y.G., Bonetti, J., 2019. Assessment of the physical vulnerability to erosion and flooding in a sheltered coastal sector: Florianópolis Bay, Brazil. *J. Coast. Conserv.* 23, 303–314. <https://doi.org/10.1007/s11852-018-0659-0>.
- Simonassi, J.C., Hennemann, M.C., Talgatti, D., Marques, A.N., 2010. Nutrient variations and coastal water quality of Santa Catarina Island, Brazil. *Biotemas* 23, 211–223.
- Smith, V.H., Schindler, D.W., 2009. Eutrophication science: where do we go from here? *Trends Ecol. Evol.* 24, 201–207. <https://doi.org/10.1016/j.tree.2008.11.009>.
- Souza, R.V. De, Campos, C., Hamilton, L., Garbossa, P., Fernando, L., Vianna, D.N., Vanz, A., Rupp, G.S., Seiffert, W., 2017. A Critical Analysis of the International Legal Framework Regulating the Microbiological Classification of Bivalve Shellfish Production Areas. , pp. 1–9. <https://doi.org/10.1111/raq.12222>.
- Strickland, J.D.H., Parsons, T.R., 1972. A Practical Handbook of Seawater Analysis. *A Pract. Handb. Seawater Anal.* vol. 167, p. 185. <https://doi.org/10.1002/iroh.19700550118>.
- Swaney, D.P., Smith, S.V., Wulff, F., 2011. The LOICZ biogeochemical modeling protocol and its application to estuarine ecosystems. *Treatise on Estuarine and Coastal Science. Elsevier*, pp. 135–159. <https://doi.org/10.1016/B978-0-12-374711-2.00907-4>.
- Team, R.C., 2015. *R: A Language and Environment for Statistical Computing*.
- Tosic, M., Restrepo, J.D., Lonin, S., Izquierdo, A., Martins, F., 2019. Water and sediment quality in Cartagena Bay, Colombia: seasonal variability and potential impacts of pollution. *Estuar. Coast. Shelf Sci.* 216, 187–203. <https://doi.org/10.1016/j.ecss.2017.08.013>.
- Vianna, L.F. de N., Bonetti, J., 2018. Spatial analysis for site selection in marine aquaculture: an ecosystem approach applied to Baía Sul, Santa Catarina, Brazil. *Aquaculture* 489, 162–174. <https://doi.org/10.1016/j.aquaculture.2017.12.039>.
- Vollenweider, R.A., Giovanardi, F., Montanari, G., Rinaldi, A., 1998. Characterization of the trophic conditions of marine coastal waters with special reference to the NW Adriatic sea: proposal for a trophic scale, turbidity and generalized water quality index. *Environmetrics* 9, 329–357.
- Wedekin, L., Daura-Jorge, F., Piacentini, V., Simões-Lopes, P., 2007. Seasonal variations in spatial usage by the estuarine dolphin, *Sotalia guianensis* (van Bénédén, 1864) (Cetacea: Delphinidae) at its southern limit of distribution. *Brazilian J. Biol.* 67, 1–8. <https://doi.org/10.1590/S1519-69842007000100002>.
- Whitfield, M., 1974. The hydrolysis of ammonium ions in sea water—a theoretical study. *J. Mar. Biol. Assoc. United Kingdom* 54, 565–580. <https://doi.org/10.1017/S002531540002275X>.
- Wilkinson, F.P., Dugdale, R.C., Marchi, A., Collins, C.A., 2002. Hydrography, nutrients and chlorophyll during El Niño and La Niña 1997–99 winters in the Gulf of the Farallones, California. *Prog. Oceanogr.* 54, 293–310. [https://doi.org/10.1016/S0079-6611\(02\)00055-1](https://doi.org/10.1016/S0079-6611(02)00055-1).
- Wolter, K., Timlin, M.S., 2011. El Niño/Southern Oscillation behaviour since 1871 as diagnosed in an extended multivariate ENSO index (MEI.ext). *Int. J. Climatol.* 31, 1074–1087. <https://doi.org/10.1002/joc.2336>.
- Xu, H., Wolanski, E., Chen, Z., 2013. Suspended particulate matter affects the nutrient budget of turbid estuaries: modification of the loicz model and application to the yangtze estuary. *Estuar. Coast. Shelf Sci.* 127, 59–62. <https://doi.org/10.1016/j.ecss.2013.04.020>.
- Zeldis, J.R., Swaney, D.P., 2018. Balance of catchment and offshore nutrient loading and biogeochemical response in four New Zealand coastal systems: implications for resource management. *Estuar. Coasts* 41, 2240–2259. <https://doi.org/10.1007/s12237-018-0432-5>.
- Zimmer-Faust, A.G., Brown, C.A., Manderson, A., 2018. Statistical models of fecal coliform levels in Pacific Northwest estuaries for improved shellfish harvest area closure decision making. *Mar. Pollut. Bull.* 137, 360–369. <https://doi.org/10.1016/j.marpolbul.2018.09.028>.